

University of Kentucky

UKnowledge

Theses and Dissertations--Earth and
Environmental Sciences

Earth and Environmental Sciences

2015

DYNAMIC SURFACE WATER-GROUNDWATER EXCHANGE IN TIDAL FRESHWATER ZONES: INSIGHTS FROM THE CHRISTINA RIVER BASIN (DELAWARE, USA)

Cole T. Musial

University of Kentucky, ctmusial@gmail.com

[Right click to open a feedback form in a new tab to let us know how this document benefits you.](#)

Recommended Citation

Musial, Cole T., "DYNAMIC SURFACE WATER-GROUNDWATER EXCHANGE IN TIDAL FRESHWATER ZONES: INSIGHTS FROM THE CHRISTINA RIVER BASIN (DELAWARE, USA)" (2015). *Theses and Dissertations--Earth and Environmental Sciences*. 28.

https://uknowledge.uky.edu/ees_etds/28

This Master's Thesis is brought to you for free and open access by the Earth and Environmental Sciences at UKnowledge. It has been accepted for inclusion in Theses and Dissertations--Earth and Environmental Sciences by an authorized administrator of UKnowledge. For more information, please contact UKnowledge@lsv.uky.edu.

STUDENT AGREEMENT:

I represent that my thesis or dissertation and abstract are my original work. Proper attribution has been given to all outside sources. I understand that I am solely responsible for obtaining any needed copyright permissions. I have obtained needed written permission statement(s) from the owner(s) of each third-party copyrighted matter to be included in my work, allowing electronic distribution (if such use is not permitted by the fair use doctrine) which will be submitted to UKnowledge as Additional File.

I hereby grant to The University of Kentucky and its agents the irrevocable, non-exclusive, and royalty-free license to archive and make accessible my work in whole or in part in all forms of media, now or hereafter known. I agree that the document mentioned above may be made available immediately for worldwide access unless an embargo applies.

I retain all other ownership rights to the copyright of my work. I also retain the right to use in future works (such as articles or books) all or part of my work. I understand that I am free to register the copyright to my work.

REVIEW, APPROVAL AND ACCEPTANCE

The document mentioned above has been reviewed and accepted by the student's advisor, on behalf of the advisory committee, and by the Director of Graduate Studies (DGS), on behalf of the program; we verify that this is the final, approved version of the student's thesis including all changes required by the advisory committee. The undersigned agree to abide by the statements above.

Cole T. Musial, Student

Dr. Audrey Hucks Sawyer, Major Professor

Dr. Edward W. Woolery, Director of Graduate Studies

DYNAMIC SURFACE WATER-GROUNDWATER EXCHANGE IN TIDAL FRESHWATER
ZONES: INSIGHTS FROM THE CHRISTINA RIVER BASIN (DELAWARE, USA)

THESIS

*A thesis submitted in partial fulfillment of the
requirements for the degree of Master of Science in the
College of Arts and Sciences
at the University of Kentucky*

By

Cole Thomas Musial

Lexington, Kentucky

Director: Dr. Audrey Hucks Sawyer, Assistant Professor of Earth and Environmental

Science

Lexington, Kentucky

2015

Copyright © Cole Thomas Musial, 2015

ABSTRACT OF THESIS

DYNAMIC SURFACE WATER-GROUNDWATER EXCHANGE IN TIDAL FRESHWATER ZONES: INSIGHTS FROM THE CHRISTINA RIVER BASIN (DELAWARE, USA)

In coastal rivers, tides can propagate for tens to hundreds of kilometers inland beyond the saltwater line. Yet the influence of tides on river-aquifer connectivity and solute transport in tidal freshwater zones (TFZs) is largely unknown. We estimate that along the TFZ of White Clay Creek (Delaware, USA), more than 17% of river water exchanges through hyporheic and riparian storage zones due to tidal pumping alone. Additional hyporheic processes such as flow through bedforms likely contribute even more exchange. The turnover length associated with the tidal pumping process is 39 km, similar to turnover lengths for all hyporheic exchange processes in non-tidal rivers of similar size. Based on measurements at a transect of piezometers located 17 km from the coast, tidal pumping exchanges 0.44 m^3 of water across the bank and 0.49 m^3 across the bed per unit river length. Exchange fluxes range from -0.81 to 1.68 m d^{-1} across the bank and -0.84 to 1.88 m d^{-1} across the bed. During rising tide, river water infiltrates into the riparian aquifer, and the downstream transport rate in the channel is low ($1.45 \text{ m}^3 \text{ s}^{-1}$). During falling tide, stored groundwater is released to the river, and the downstream transport rate in the channel increases by 380%. Tidal bank storage zones may remove nutrients or other contaminants from river water and attenuate nutrient loads to coasts. Alternating expansion and contraction of aerobic zones in the riparian aquifer likely influence contaminant removal along flow paths. A clear need exists to understand contaminant removal and other ecosystem services in TFZs and adopt best management practices to promote these ecosystem services.

KEYWORDS: Hyporheic exchange, bank storage, tidal freshwater zone, coastal processes, tidal pumping

Cole Thomas Musial

March 27, 2015

DYNAMIC SURFACE WATER-GROUNDWATER EXCHANGE IN TIDAL FRESHWATER
ZONES: INSIGHTS FROM THE CHRISTINA RIVER BASIN (DELAWARE, USA)

By

Cole T. Musial

Audrey H. Sawyer
Director of Thesis

Edward W. Woolery
Director of Graduate Studies

March 27, 2015
Date

ACKNOWLEDGMENTS

First and foremost, I would like to thank my thesis advisor, Dr. Audrey H. Sawyer, who provided me the opportunity to work in an amazing field area and on a challenging but gratifying project. I will be forever grateful for this.

I would also like to thank my thesis committee members, Dr. Alan Fryar and Dr. Kevin Yeager, for serving on my committee, and the various other UK EES faculty members for their teachings throughout my graduate career. Additionally I appreciate the support and guidance of the department staff, Kim Schindler, Peter Idstein and Adrienne Gilley.

Many hands make light work, and I'm grateful for the help that Deon Knights, Sam Bray, Chris Russoniello, and Kaileigh Calhoun provided me in the field. Additionally, I want to thank Ralph and Kim Burdick provided us with access to our field site and support for this project. Stroud Water Research Center, Anthony Aufdenkampe, Louis Kaplan, and many others that were gracious in allowing us access to their field equipment, time and advice throughout the field season. Holly Michael allowed us use of both her equipment and graduate students. Last but not least, I want to thank Rebecca Barnes whose help in the field and advice throughout this project provide numerous helpful insights for my thesis.

Without the proper funding this project would have not been successful. I would like to thank the GSA Student Research Grant, the Ferm and Brown-McFarlan funds of the UK Department of Earth and Environmental Sciences for helping cover field expenses, and GSA additionally for providing me with funding to travel to the 2014 Annual Meeting to present the work described here.

TABLE OF CONENTS

Acknowledgements.....	iii
Table of Contents.....	iv
Table of Figures.....	vii
Chapter 1. Introduction.....	1
Chapter 2. Study Area.....	3
Chapter 3. Methods.....	7
3.1. Aquifer Characterization.....	7
3.2 Measurement of Groundwater and Hyporheic Dynamics.....	8
3.3 Measurement of River Discharge Dynamics.....	10
Chapter 4. Results.....	12
4.1. Hydrostratigraphy.....	12
4.2 Surface Water Dynamics.....	14
4.3 Surface Water-Groundwater Interactions.....	14
4.4 River and Groundwater Quality.....	16
Chapter 5. Discussion.....	23
5.1 Insights from White Clay Creek.....	23
5.2 Bank Filtration: An analogous process.....	28
5.3 Conceptual Model of Solute Transport in TFZs.....	39
5.4 Suggestions for Best Management of TFZs.....	30
Chapter 6. Conclusions.....	36
Appendix A. Grain Size Analysis.....	37
Appendix B. Grain Size Distributions.....	38
Appendix C. Low Tide Groundwater and Surface Water Chemistry Parameters.....	41
Appendix D. High Tide Groundwater and Surface Water Chemistry Parameters.....	42

Appendix E. Piezometer Data.....	43
Appendix F. Field Photographs.....	44
Appendix G. Water Table Fluctuation Logs.....	46
References.....	47
CURRICULUM VITA.....	52

TABLE OF FIGURES

Figure 2.1 Regional Field Site Location.....	5
Figure 2.2 Field Site Layout and Geology.....	6
Figure 3.1 Time Table of Measurements.....	11
Figure 4.1 Hydraulic Conductivity Histogram and Cumulative Grain Size Distributions	18
Figure 4.2 Stream Velocity Contours and Discharge-Stage Relationship.....	19
Figure 4.3 Water Table Fluctuations and Darcy Flux.....	20
Figure 4.4 Streambed Vertical Head Gradients.....	21
Figure 4.5 Water Quality Cross Sections.....	22
Figure 5.1 Turnover Length Concept.....	32
Figure 5.2 Hydraulic Retention Concept.....	33
Figure 5.3 Turnover Length Comparison.....	34
Figure 5.4 Conceptual Model of Surface Water-Groundwater Dynamics.....	35

Chapter 1. Introduction

The mixing of river water and groundwater, or hyporheic exchange, influences the fate of nutrients, contaminants and dissolved organic matter in watersheds (*Brunke and Gonser, 1997; Stanford and Ward, 1988*). Hyporheic exchange exposes river water to microbially active sediment, providing opportunities for biogeochemical transformation of solutes (*Findlay, 1995*). Hyporheic exchange can be driven by multiple mechanisms. Current interactions with bedforms (*Thibodeaux and Boyle, 1987; Packman et al., 2004; Boano et al., 2007*) and meanders (*Boano et al., 2006; Kasahara and Hill, 2007*) create pressure gradients along the sediment-water interface that induce exchange. Permeability heterogeneity also enhances exchange by deflecting flow upward or downward in the bed (*Woessner, 2000; Cardenas et al., 2004; Packman et al., 2006*). Bank storage and release represents another form of hyporheic exchange. Bank storage can occur due to storms (*Pinder and Sauer, 1971; Bates et al., 2000*), dam releases (*Francis et al., 2010; Sawyer et al., 2009*), and snowmelt cycles (*Loheide and Lundquist, 2009*). Tides also drive semidiurnal bank storage in coastal rivers and creeks (*Wilson and Gardner, 2006; Xin et al., 2011*). I hypothesize that bank storage in tidal freshwater zones can generate magnitudes of hyporheic exchange similar to other hyporheic processes.

Tides extend inland from the coast for tens to hundreds of kilometers in unregulated rivers. The region above the salt wedge where river stage still fluctuates is called the tidal freshwater zone (TFZ) (*Schuchardt et al., 1993*). Large tidal stage fluctuations in TFZs should drive significant bank storage, which may influence the downstream transport of nutrients and other contaminants. Yet, few studies have examined hyporheic exchange or the fate of solutes in TFZs. *Bianchin et al. (2011)* found that tides increased the depth of hyporheic mixing in the TFZ of the Fraser River (British

Columbia, Canada). Over a single tidal cycle, river water typically penetrated 15 cm into the bed, and enhanced dispersion further increased the depth of solute exchange to 1 m. Polycyclic aromatic hydrocarbons (PAHs) in groundwater were found to be degraded by aerobic bacteria within the hyporheic zone, reducing concentrations to nondetectable levels near the channel (*Bianchin et al.*, 2010). In the TFZ of the Newport River (North Carolina), *Ensign et al.* (2008) showed that overbank flooding during high tide enhanced denitrification in floodplain sediments. The influence of these hydrologic and geochemical dynamics on downstream water quality remains largely unknown.

In non-tidal rivers, stage fluctuations and bank storage clearly alter water quality (*Valett et al.*, 1996). *Anderson et al.* (2011) studied heat transport during storms in urban watersheds and showed that bank storage decreases stream temperatures and attenuates heat pollution from urban runoff. In an agricultural stream, bank storage was shown to mobilize atrazine, an herbicide, in a riparian aquifer and release it to the stream (*Squillance et al.*, 1993). In a regulated river subject to frequent dam releases, bank storage diluted inputs of uranium from the surrounding aquifer (*Fritz and Arntzen* 2007). Bank storage may also alter fluxes of nitrate from groundwater to rivers. Under base flow conditions, groundwater-borne nitrate is typically reduced as groundwater flows through organic-rich sediments in the riparian aquifer (*Bohlke and Denver*, 1995; *Rivett et al.*, 2008; *Hill et al.*, 2000). During bank storage events, groundwater residence times temporarily increase, which extends groundwater contact time with microbially active organic-rich sediments and may increase removal of groundwater-borne nitrate. *Gu et al.* (2012) showed that bank storage zones are also capable of removing river-borne nitrate. Models of reactive nitrogen transport over multiple storm events showed that bank

storage zones remove five times more nitrate from surface water than traditional streambed storage zones on an annual basis. Nitrate is an important contaminant in coastal rivers, since it is often the limiting nutrient that drives eutrophication of coastal waters (*Ryther and Dunstan, 1971; Turner and Nancy, 1994*). Bank storage in TFZs may be critical for reducing nitrogen loads to coasts.

Given the increasing pressures on TFZs from sea level rise (*IPCC, 2014*) and dam construction (*Graf 2006*), it is imperative to understand physical processes that control the biogeochemical transformation potential of TFZs. My objectives were to quantify hyporheic exchange associated with bank storage and characterize potential implications for surface water and groundwater quality. I selected a representative transect based on surficial geology within an incised TFZ where I monitored hydraulic head over multiple tidal cycles and measured basic water quality parameters (specific conductivity, pH, DO) in surface water, hyporheic water, and riparian groundwater. I first present observations from my TFZ transect. Next, I offer a conceptual model for the influence of river-groundwater interactions on organic contaminant transport and degradation in TFZs. Finally, I suggest best management strategies for TFZs that are intended to promote river-aquifer connectivity and ecosystem services such as contaminant processing. I demonstrate that tidal bank storage within TFZs enhances hydrologic retention and may play an important role in transforming contaminants in surface water or groundwater.

Chapter 2. Study Area

The field site is located in the TFZ of White Clay Creek (39.701172°,-75.649987°), a fifth-order river near Wilmington, Delaware (USA), within the Christina River Basin Critical Zone Observatory (Figure 2.1). The Christina River Basin Critical Zone Observatory is one of ten established critical zone observatories in the United

States. Land use within the 277 km² watershed is predominantly agricultural and suburban but additionally includes mature forests and commercial. The site lies 16.9 river km from the Delaware river (Figure 2.1). River water remains fully fresh, but tides fluctuate by almost a meter twice daily.

The channel of White Clay Creek is generally incised (Figure 2.2), and floodplains remain exposed at high tide similar to other large coastal rivers such as the Fraser River, British Columbia (*Bianchin et al., 2011*). Floodplain connectivity is unlike smaller first-order tidal creeks in coastal marshes where the floodplain is inundated at high tide (*Ensign et al., 2008; Moffett et al., 2012; Wilson and Gardner, 2006*). Within the channel of White Clay Creek, alternating sandy point bars are common. The primary study transect spans one such point bar and the adjacent floodplain of the eastern bank (Figure 2.2). Surficial geology is characterized as alluvial at the field site and is the primary geology upriver (*Ramsey 2005*). Downriver, surficial geology is a mix between marsh deposits, fill, and sand deposits (*Ramsey 2005*). Land use on this bank was agricultural during colonial times but has since returned to forest (Kim Burdick, personal communication). The western bank was not instrumented because it has been reinforced with extensive rip rap. A secondary transect was also established 20 m downstream to examine longitudinal variations in surface water-groundwater interactions (Figure 2.2a).

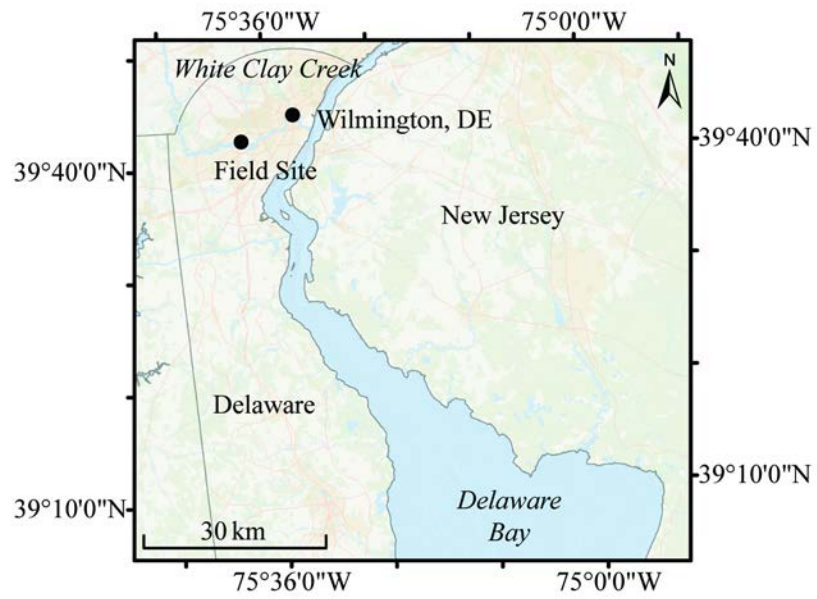


Figure 2.1. The field site is located on White Clay Creek in Delaware (USA), 17 km upstream from the Delaware River.

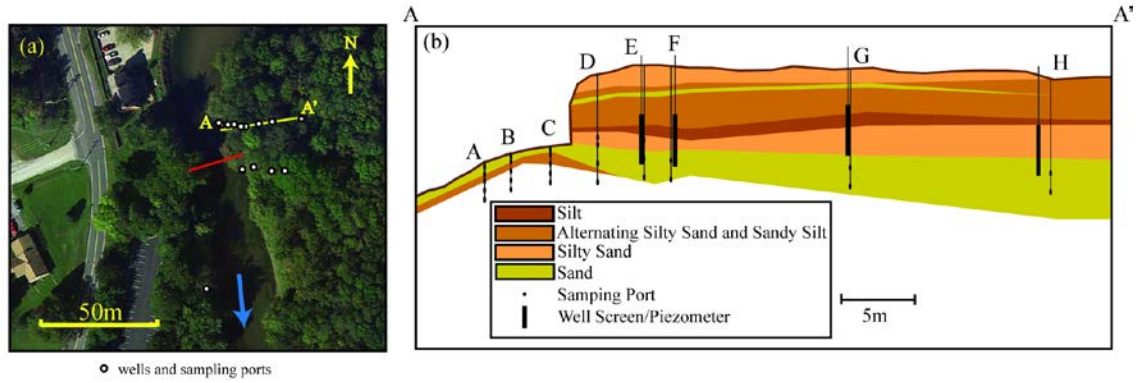


Figure 2.2. (a) Aerial image (courtesy of Google Earth 2015) and (b) cross section of transect in the tidal freshwater zone of White Clay Creek, Christina River Basin Critical Zone Observatory (Delaware, USA). Vertical exaggeration in panel (b) is 2.5 and the blue arrow refers to downstream flow.

Chapter 3. Methods

3.1. Aquifer Characterization

Eight cores (2.54 cm outer diameter [o.d.]) were taken along the primary transect to constrain floodplain and riverbed hydrostratigraphy and sediment properties. Six cores were from the floodplain and two were from the channel point bar. Cores were collected using an AMS Sand Sludge Sediment Probe with multiple extensions. Cores were immediately sealed and refrigerated until the end of the field season, when they were transported on ice to the University of Kentucky.

Cores were visually described for grain size, color, and composition at 1 cm resolution. Based on visual descriptions, thirty 2-cm intervals were selected for bulk density (BD), porosity, and grain size analysis from one representative riverbed core and one representative floodplain core (Locations B and F, Figure 2.2b). Cores were deemed representative based on horizontal continuity from descriptions and location near the region of exchange. Samples for BD and porosity were collected from intact cores using a 1 ml syringe. Because samples spanned the unsaturated and saturated zones, porosity was estimated independently from BD based on plug dry weight and plug volume. Sediments from the 2-cm interval surrounding each plug were analyzed for grain size. All eight cores were sectioned into 2 cm intervals for archive.

Grain size was analyzed using a Malvern Mastersizer 2000 for sediments within the range of 0.02-2000 μm . Larger grains were removed by sieving and weighed prior to analysis. Only three of the thirty samples contained larger grains. Hydraulic conductivity (K) was determined from grain size distributions based on the empirical Hazen equation (Hazen, 1893):

$$K = C(d_{10})^2, \quad (1)$$

where C ($\text{s}^{-1} \text{cm}^{-1}$) is a coefficient based on sediment type (*Fetter, 2001*) and d_{10} is the effective grain size (cm). Sediment type was determined based on its textural classification and sorting from visual descriptions. Hydraulic conductivity estimates from the Hazen method have been shown to agree well with estimates from other methods at a similar site that was primarily comprised of sands (*Schultz and Ruppel, 2002*). I did not attempt to estimate hydraulic conductivity from slug tests in the field, which would have required the use of a packer, since piezometers were screened through the water table.

3.2. Measurement of Groundwater and Hyporheic Dynamics

Six bank piezometers and one river stage recorder were installed along the primary transect to monitor lateral bank storage and release (Figure 2.2, piezometers D through H). Four additional piezometers were installed at the secondary transect downstream to constrain longitudinal variations in bank storage (Figure 2.2a). Bank piezometers were constructed of PVC with 4.5 cm o.d. and were screened through the zone of water table fluctuations. The screen interval for all bank piezometers was 1.36 m. River stage was additionally monitored with a stilling well by anchoring a 1.36 m screened PVC section to a 1.57 m section of casing inserted in the riverbed. Pressure sensors (In-Situ Aqua Troll 200s and Schlumberger Divers) were installed in all piezometers and were programmed to sample at 15-minute intervals from June 15 to June 30, 2014 (Figure 3.1). Rates of bank storage and release were calculated using Darcy's law between the riparian aquifer and river using piezometer D (Figure 2.2).

To monitor groundwater quality, thirteen sampling ports were installed next to piezometers at depths between 1.8 and 3 m below ground surface (Figure 2.2). Bank ports were installed using an AMS Gas Vapor Probe kit. Individual ports were

constructed of a gas vapor tip, fluoropolymer umbrella, and 2 cm #50 screen mesh connected to 0.635 cm o.d. polypropylene tubing.

Three in-stream piezometer nests were installed in the point bar of the primary transect to quantify vertical exchange and sample pore water from the riverbed (Figure 2.2, piezometer nests A, B, and C). Nests were constructed of 0.635 cm o.d. polypropylene tubing strapped to 1.27 cm PVC risers. Tubes were perforated over a 2-cm interval and covered with 50 μm nylon mesh. Each nest had ports at 12, 25, 50, 75 and 100 cm below the riverbed. Nest C was only inundated at high tide, nest B was mostly inundated over the tidal cycle, and nest A was always inundated. Differences in hydraulic head between each of the deepest ports (100 cm) and river were measured manually using a manometer board at 15-minute intervals on June 18, 2014 (Figure 3.1). Vertical head gradients (VHG) were used to calculate exchange rates across the riverbed based on Darcy's law. All piezometers and bank topography were surveyed using a Nikon NPL 362 Total Station.

On June 16, 2014, I measured basic water quality (specific conductivity, temperature, pH, and dissolved oxygen) during low and high tide at all ports in the bed and banks (Figure 3.1). The multimeter was calibrated the morning of June 16, 2014. Pore water was extracted using a peristaltic pump at a slow rate (~ 50 mL/min) to minimize disturbance to hydraulic gradients. One tubing volume was first discarded (60 mL), and then pore water was pumped into a 70 mL container. Field parameters were measured with a Thermo Orion Star A3229 while overflowing the container to minimize oxygen transfer from the atmosphere.

3.3. Measurement of River Discharge Dynamics

To monitor tidal surface water dynamics, river discharge was measured using a Teledyne RDI StreamPro Acoustic Doppler Current Profiler at 1-hour intervals on June 18, 2014 (Figure 3.1). The transect for river discharge measurements was located between the primary and secondary piezometer transects (Figure 2.2). Although river discharge and other manual measurements such as water quality were made on three separate days, I assume that tidal dynamics did not change significantly over the window of measurements because river stage fluctuations remained approximately constant (Figure 3.1). In other words, I assume that river discharge measurements on June 18, 2014, were representative of discharge dynamics on the day of water quality measurements (June 16, 2014) and vice versa. Significant rainfall occurred over June 10, 2014 to June 13, 2014, but water table fluctuations had returned to base flow conditions by June 16, 2014 (NOAA). Rainfall can be seen to have occurred in Figure 3.1 on June 19, 2014, but data collection had been completed at this point. From June 19, 2014 to June 30, 2014 only water table logs were collected.

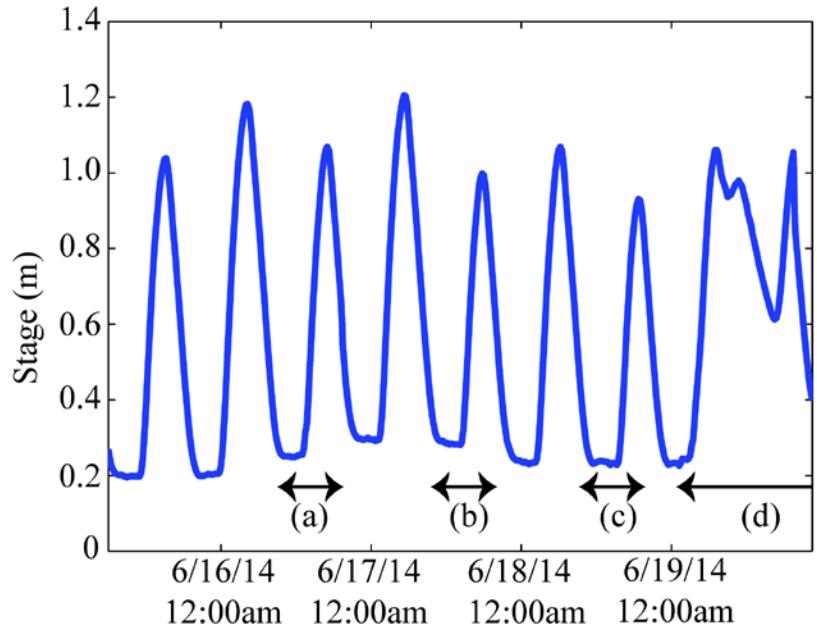


Figure 3.3.1. Stream stage fluctuations were generally consistent during the study interval until June 19th, when rain fell. Pore water was sampled June 16th (a), and stream discharge and manometer readings were made on June 18th (c). Hydrologic monitoring at the second transect began on June 19th and continued until June 30th (d).

Chapter 4. Results

4.1. Hydrostratigraphy

Riverbed and floodplain deposits generally consist of a lower sand unit overlain by silt and sand layers (Figure 2.2b). The lower sand unit is light tan (10YR 6/6) to medium brown (7.5YR 3/3) in color with some orange (5YR 5/6) oxidation staining. Grains are predominantly quartz with some potassium feldspar and micaceous minerals including muscovite and biotite. Compositions were determined by visual identification using an Olympus SZX14 microscope. These sediments are poorly sorted, ranging from pea gravel to very fine sand with trace amounts of clay. The three grain size samples from the lower sand unit contain on average 24.4 % by volume of gravel (Figure 4.1). Average bulk density is 2.34 g cm^{-3} (range [R]: 2.19-2.50, standard deviation [SD]: 0.1, median [MED]: 2.37), and porosity is 0.49 (R: 0.38-0.55, SD: 0.07, MED: 0.46). Average hydraulic conductivity is 0.0015 m s^{-1} (R: 2.66×10^{-5} - 2.98×10^{-3} , SD: .001, MED: 1.78×10^{-3}), typical of unconsolidated sand (*Freeze and Cherry, 1979*). The recovered thickness of the lower sand unit was only ~100 cm, but the full thickness is unknown, since cores did not penetrate the base. The lower sand unit is overlain by a silty sand facies that is light brown (7.5YR 4/6) in color. Grains are predominantly quartz with some potassium feldspar and muscovite. Grains are poorly sorted and include occasional pea gravel. Average bulk density is 2.31 g cm^{-3} (R: 2.31-2.41, SD: 0.05, MED: 2.32) and porosity is 0.42 (R: 0.41-0.64, SD: 0.12, MED: 0.47). The average hydraulic conductivity is $2.17 \times 10^{-4} \text{ m s}^{-1}$ (R: 2.2×10^{-5} - 1.63×10^{-4} , SD: .0001, MED: 1.09×10^{-4}), and average thickness is 50 cm. Hydraulic conductivity is comparable to published values from *Fetter (2001)*. The silty sand facies is overlain by a relatively impermeable silt facies. Silts are dark grey (2.5Y 4/1) with orange staining (5YR 5/6) and are moderately sorted. The average bulk

density is 2.32 g cm^{-3} , average porosity is 0.44, and average hydraulic conductivity is $1.46 \times 10^{-5} \text{ m s}^{-1}$. Hydraulic conductivity is comparable to published values for silts (10^{-4} - 10^{-5}) from *Fetter* (2001). The silt facies is 26 cm thick on average and may act as a partially confining unit at high tide. The silt facies is overlain by a unit of alternating silty sand and sandy silt that is approximately 75 cm thick. Individual layers are approximately 10 cm thick and generally alternate from tan (10YR 6/6) silty sand to medium brown (7.5YR 3/3) sandy silt. Sorting is moderate within individual beds, and macroscopic organic matter occurs sporadically throughout the facies. Average bulk density is 2.36 g cm^{-3} (R: 2.31-2.41, SD: 0.05, MED: 2.32), and porosity is 0.44 (R: 0.27-0.53, SD: 0.08, MED: 0.41). The average hydraulic conductivity is $2.45 \times 10^{-4} \text{ m s}^{-1}$ (R: 2.37×10^{-4} - 1.22×10^{-3} , SD: .00033, MED: 1.96×10^{-4}), very similar to the published range of silty sands (10^{-5} - 10^{-3}) by *Fetter* (2001). The alternating silty sand and sandy silt facies includes one relatively thick sand unit of similar composition to the lower sand unit but lacking pea gravel. The floodplain sequence is capped by a silty sand unit of similar composition to the lower silty sand unit (Figure 2.2b).

I estimate that the effective hydraulic conductivity is $1.41 \times 10^{-3} \text{ m s}^{-1}$ for the saturated floodplain aquifer sequence and $1.09 \times 10^{-3} \text{ m s}^{-1}$ for the riverbed sequence (Figure 4.1). The floodplain aquifer value was calculated using the harmonic average of the saturated units (lower sand and silty sand facies), since flow in the floodplain aquifer is primarily horizontal along hydrostratigraphic units. The riverbed value was calculated using the arithmetic average, since flow across the riverbed is primarily vertical across hydrostratigraphic units.

Cores were not taken at the secondary transect, but sediments were observed to have a substantially higher silt fraction during piezometer installation. I did not encounter the lower sand unit at the secondary transect, either because it lay below the maximum core depth or was locally absent.

4.2. Surface water dynamics

Tides fluctuated semidurnally with an average amplitude of 0.75 m over the monitoring period (Figure 3.1). River velocity fluctuated with tides but never reversed. During rising tide, velocity decreased (Figure 4.2a). During falling tide, velocity increased (Figure 4.2b). Changes in velocity were greatest within the thalweg of the river. Minimal fluctuation occurred along channel margins and over point bars, which exhibited consistently slow velocities.

The stage-discharge relationship was hysteretic (Figure 4.2c). At low tide, discharge was moderate ($4.6 \text{ m}^3 \text{ s}^{-1}$). As tide rose, discharge initially decreased with river velocity. The lowest discharge ($1.45 \text{ m}^3 \text{ s}^{-1}$) occurred around 1.5 hours before high tide. River discharge then increased as tide continued to rise. At high tide, river discharge was similar to values at low tide ($4.6 \text{ m}^3 \text{ s}^{-1}$). As tide fell, river discharge continued to increase with river velocity. Peak discharge ($6.96 \text{ m}^3 \text{ s}^{-1}$) occurred 1.5 hours after high tide. As stage continued to fall, discharge declined again. Average discharge over a single tidal cycle was $4.33 \text{ m}^3 \text{ s}^{-1}$.

4.3 Surface water-groundwater interactions

Water table elevation fluctuated with tides, and the amplitude of fluctuations decreased with distance into the riparian aquifer (Figure 4.3a). At the primary transect,

amplitudes were 91%, 57%, 48%, and 11% of the river stage amplitude for piezometers E through H, respectively. At the second transect (not shown), amplitudes of water table fluctuations were comparatively much smaller (14%, 8%, 5% and 0.1%, in order of increasing piezometer distance from the river). During low tide, hydraulic head in the bank sloped toward the river (groundwater discharged to the river). As tide increased, hydraulic head gradients decreased and then reversed. Infiltration into the bank began approximately 3 hours after the start of rising tide and spanned approximately 2 hours. Based on Darcy's Law where q is specific discharge, K is hydraulic conductivity (m s^{-1}), and dh/dl is the hydraulic gradient, the instantaneous flow rate across the bank ranged from -0.81 to 1.68 m d^{-1} during the three-day period of intensive monitoring (Figure 4.3b):

$$q = -K \frac{dh}{dl}. \quad (2)$$

The total bank storage volume was 0.44 m^3 per tidal cycle per meter of bank, and the average net flux per tidal cycle was 0.43 m^3 per unit area of bank (or 0.98 m/d), indicating net gaining conditions.

Vertical head differences in the riverbed also fluctuated with tides (Figure 4.4) except at the centermost piezometer A, where the head difference was consistently positive. At piezometers B and C during low tide, vertical head differences were positive, and flow was upward. With rising tide, the switch to losing conditions (infiltration) occurred almost instantly. Tidal hyporheic storage spanned approximately 4.25 hours. During falling tide, the hydraulic gradient again reversed (Figure 4.4), indicating a return to upward flow and gaining conditions. Fluxes ranged from -0.66 to 0.38 m d^{-1} at

piezometer B and -0.81 to 1.88 m d⁻¹ at piezometer C. The total hyporheic storage volume was 0.49 m³ per tidal cycle. Net flux per tidal cycle was -0.05 m³ at piezometer B and 0.04 m³ at piezometer C (-0.09 m/d and 0.11 m/d, respectively).

4.4 River and Groundwater quality

At low tide (11:30), specific conductivity in the river was 351.8 $\mu\text{S cm}^{-1}$, pH was 7.69, and the DO concentration was 8.75 mg L⁻¹. River parameters were similar at high tide (15:30), with specific conductivity essentially unchanged (351.2 $\mu\text{S cm}^{-1}$), pH slightly lower (7.54), and DO slightly higher (9.04 mg L⁻¹). The lower pH and higher DO are likely associated with photosynthetic activity.

Specific conductivity, pH, and DO in pore water were generally lower than river water (Figure 4.5). Within the riverbed at low tide, specific conductivity generally decreased from 400 to 240 $\mu\text{S cm}^{-1}$ over the 1-m depth interval, pH decreased from 6.7 to 5.8, and DO decreased from 1.25 to 0.5 mg L⁻¹. In the floodplain aquifer near the riverbank (location E, Figure 4.5), water quality parameters were similar to the shallow riverbed: specific conductivity was 260 $\mu\text{S cm}^{-1}$, pH was 6.4, and DO was 0.65 mg L⁻¹. DO farther from the channel near the water table was moderately elevated (location G, Figure 4.5). I assume that the deepest port located farthest from the channel (location H, Figure 2.2) was representative of the groundwater end member, since water quality parameters at that port were more distinct from the river than most other ports, and the values did not fluctuate between low and high tide. The specific conductivity there was 251 $\mu\text{S cm}^{-1}$, pH was 5.92, and DO concentration was 0.57 mg L⁻¹ (5% of saturation at a recorded temperature of 15°C) on average.

At high tide, specific conductivity and pH increased slightly near the sediment-water interface and water table. In the shallow riverbed (< 12 cm deep), DO concentrations increased up to 15%. Near the water table at location F, DO concentrations increased by ~70%. Also in the floodplain aquifer, a plume of 300-350 $\mu\text{s cm}^{-1}$ water migrated along the sand unit approximately 4 m from the river. pH also increased in this zone from 5.9 to ~6.

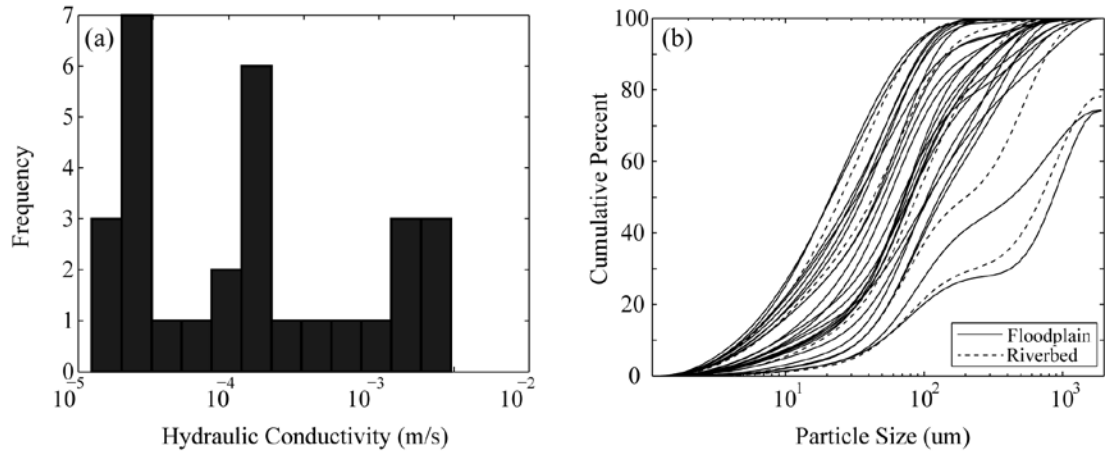


Figure 4.1. (a) Histogram of hydraulic conductivities. (b) Cumulative grain size distributions. Dashed lines indicate riverbed samples, and solid lines indicate floodplain samples.

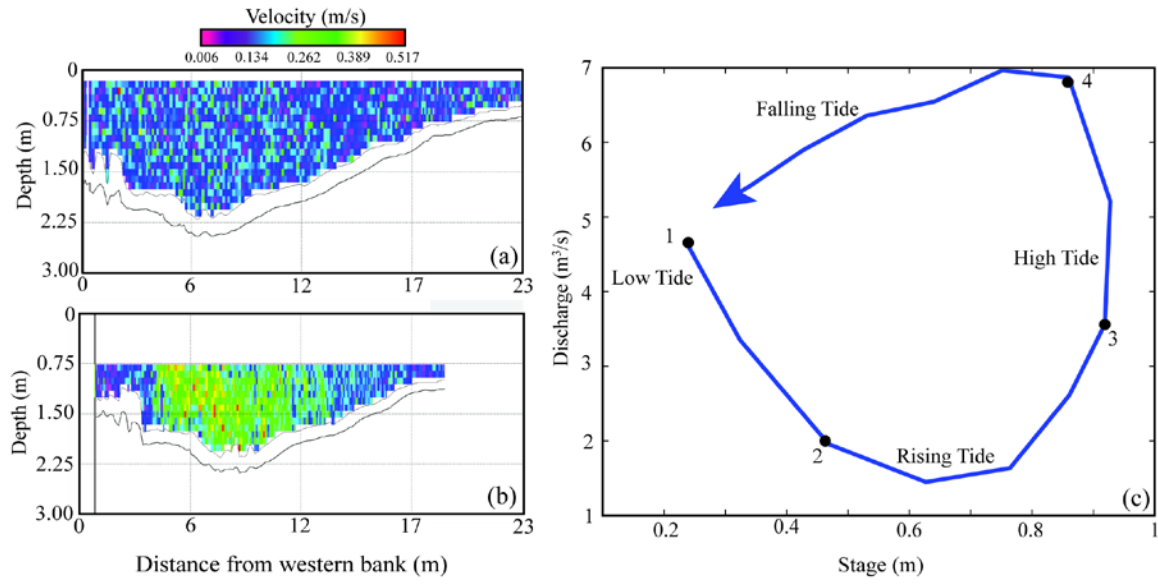


Figure 4.2. Cross section of stream velocity at (a) high tide and (b) low tide. Discharge and stage are hysteretic (c).

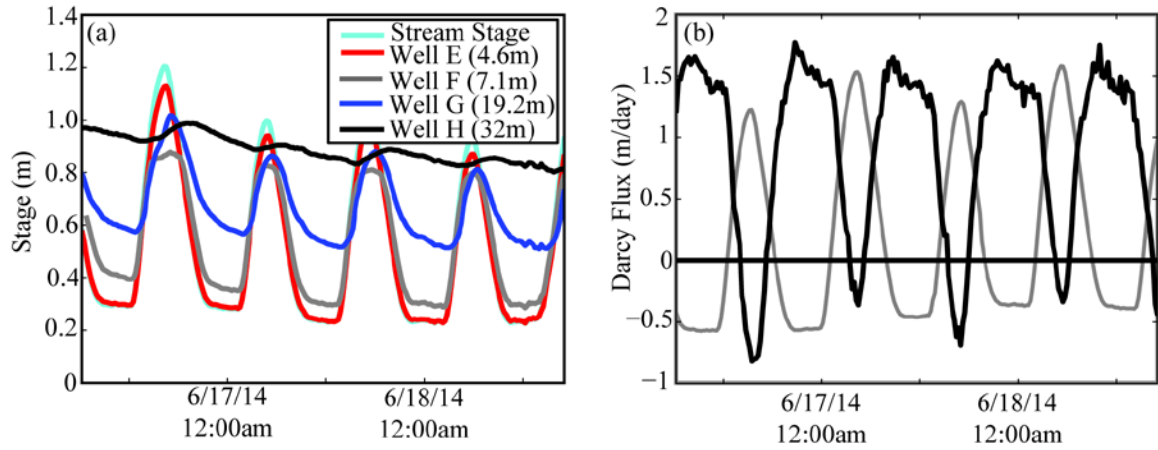


Figure 4.3. (a) Water level fluctuations in the stream and aquifer. Piezometer locations are shown in Figure 1. (b) Darcy flux (black) across the bank. Positive values denote groundwater discharge (gaining river conditions). Stream stage is shown in grey for reference.

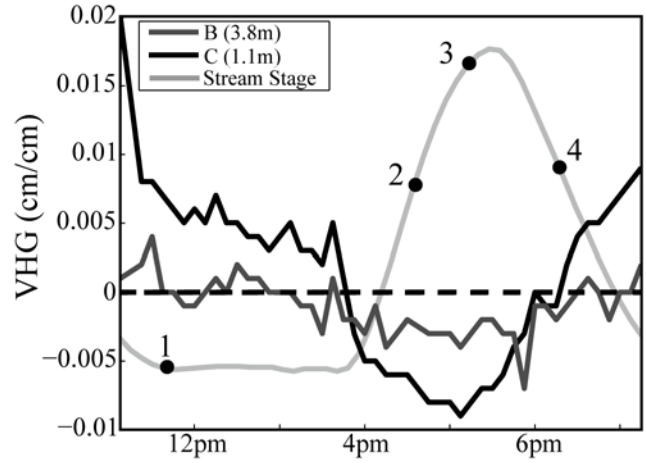


Figure 4.4. Vertical head gradients (VHG) within the stream. Positive values indicate gaining conditions (upward flow) and negative values indicate losing conditions (downward flow). VHG at piezometer A (not shown) was consistently positive and large. Stream stage is shown in gray for reference, and numbers 1-4 correspond with Figure 4.2.

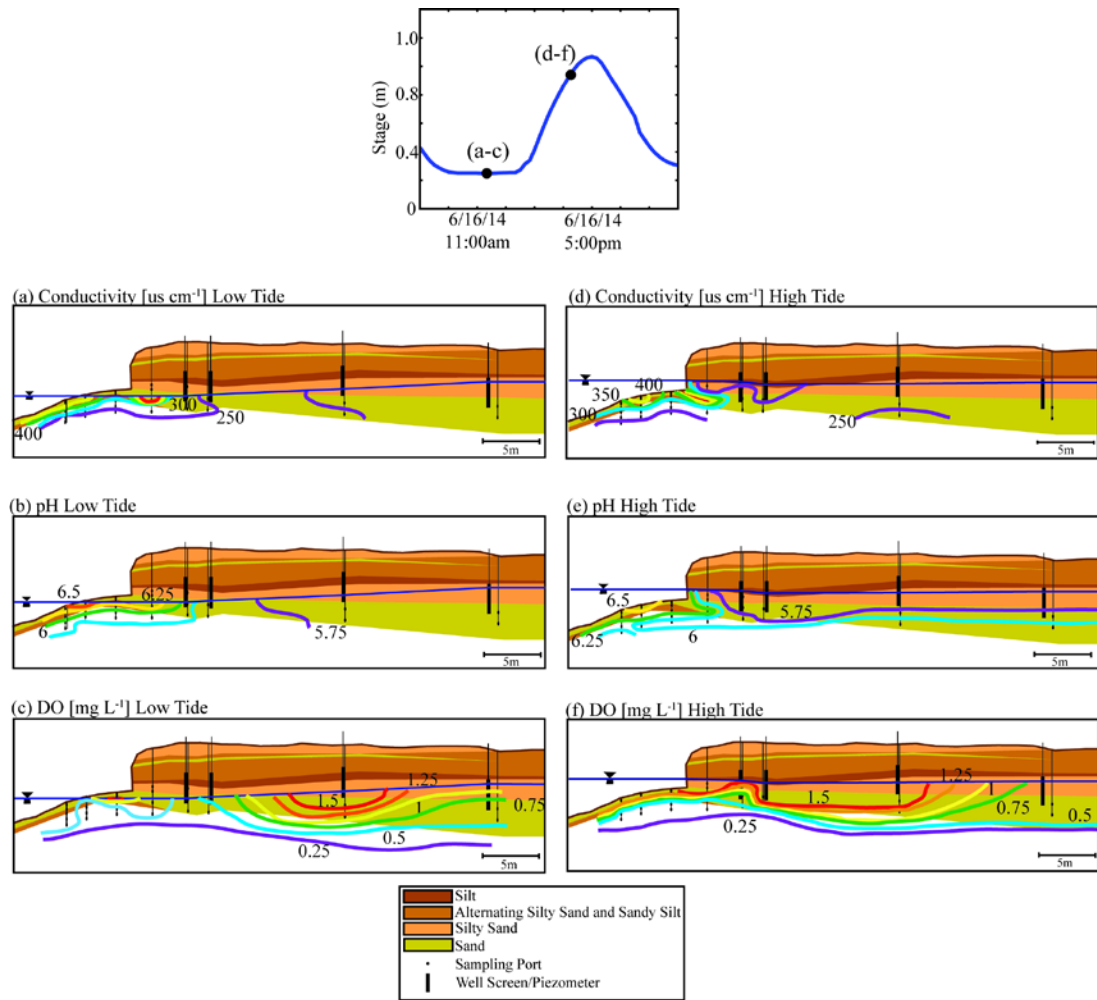


Figure 4.5. Contoured cross sections for conductivity, pH and DO at low tide (a-c) and high tide (d-f).

Chapter 5. Discussion

5.1. Insights from White Clay Creek

At this site, 17 km inland, tidal stage fluctuations alter groundwater flow and water table elevations up to 25 m from the river channel, even though tides do not inundate the floodplains. Without tides, groundwater would continuously discharge to the river. Tidal bank storage disrupts this steady discharge twice daily. I estimate that the bank storage volume is 0.44 m^3 per meter of river bank over each tidal cycle. In addition, tidal pumping across the bed contributes another 0.49 m^3 per meter of river.

Longitudinal variations in stratigraphy undoubtedly affect bank storage in TFZs. Bank storage was reduced at our secondary transect, given the smaller fluctuations in water table elevation that I recorded there. The secondary transect was siltier than the primary transect and was located farther from the upstream point bar. The primary transect may be representative of point bars, while the secondary transect may be representative of thalwegs. Within transects, lateral variations in floodplain and riverbed stratigraphy also influence bank storage and preferential flow patterns. Sandy layers allow river water to penetrate farther into the riparian aquifer into potentially reducing zones with little dissolved oxygen (Figure 4.5). At our primary transect, a plume of relatively high conductivity and pH preferentially recharged the aquifer at high tide through the lower sand unit (Figure 4.5b-c). Based on plume movement, the approximate travel distance of river water into the sand unit was 4 m. This lateral transport distance is substantially larger than the vertical transport distance into the bed at our site ($\sim 0.5 \text{ m}$) and in the Fraser River ($\sim 1 \text{ m}$) (*Bianchin et al., 2011*).

Given the importance of hydrostratigraphy for exchange processes, the fluxes I measured at my primary transect may be representative of a significant portion of the TFZ, but not necessarily all of it. The geology at my site is generally consistent with geologic descriptions upriver and downriver (alluvial deposits of interbedded sand, gravel, silt, and clay) (*Ramsey, 2005*). A large region of marsh deposits with organic-rich clays and silts also exists downriver near Churchman's Marsh (Figure 2.1, 39.696675°, -75.625882°). Less permeable sediments in this region may reduce surface water-groundwater exchange rates, but the larger surface area of the sediment-water interface within the marsh may also compensate for the effects of reduced permeability.

Despite this heterogeneity along the TFZ, I can use calculations at my transect to estimate the fraction of surface water that exchanges through the riverbanks and bed within the TFZ of White Clay Creek. Assuming a mean river discharge of $4.33 \text{ m}^3 \text{ s}^{-1}$, I estimate that 8% of river water cycles through bank storage zones over the 17 km distance from the study site to the Delaware River, and 9% of river water cycles through the bed due to tidal pumping. This volume is likely an underestimate of total exchange rates in the TFZ because the volume exchanged most likely increases in the downstream direction as tidal range increases. Additionally, my calculation neglects the storage volume upstream of my site because the location of the head of tides is unknown. Exchange due to flow through meanders and bedforms or other morphologic features is also unknown and has not been included in my estimated exchange rate. Turnover length (L_s) can be estimated for the TFZ of White Clay Creek as:

$$L_s = \frac{Q_r}{q_{ex}}, \quad (3)$$

where q_{ex} represents the combined exchange rates through the bed and banks per unit length of channel, and Q_r represents the river discharge (Figure 5.1.1). Turnover length is the average distance a water molecule travels in the channel before entering the storage zone (Cranswick and Cook 2015). I estimate that L_s is 39 km. Another common metric for describing river-groundwater interaction is hydraulic retention (R_h):

$$R_h = \frac{t_{res}}{L_s}, \quad (4)$$

where t_{res} is the residence time of river water in subsurface or lateral storage zones (Figure 5.1.2). Assuming an approximate 2 hour residence time, determined using the average period in which the hydraulic gradient was reversed per tidal cycle, the hydraulic retention (R_h) is 0.18 s m^{-1} . The turnover length and hydraulic retention in this TFZ due to tidal pumping are similar to the turnover length and hydraulic retention due to all hyporheic processes in similarly sized non-tidal rivers (Cranswick and Cook, 2015). Turnover length in this TFZ is slightly higher than average: using the power law regression provided by Cranswick and Cook (2015) and the average discharge of the river, turnover length would be considered average at 9 km, though values from the literature vary widely (Figure 5.1.3). Hydraulic retention is comparable to other published values for rivers of variable size. In Pinal Creek, Arizona (a 5th order stream), hydraulic retention increased from 0.2 to 8 s m^{-1} as new vegetation grew and channel friction increased (Harvey *et al.*, 2003). In a study of hydraulic retention in first order streams, Morrice *et al.*, (1997) found low retention in two streams (0.53 s m^{-1} in Aspen Creek, New Mexico and 1.5 s m^{-1} in Rio Calaveras, New Mexico) and high retention in a third stream (306 s m^{-1} in Gallina Creek, New Mexico). Climate, topography, and land use

vary and will have an impact on hydraulic retention. As more studies publish retention values, comparisons between metrics will be more meaningful for given climates, topographies and land uses.

These comparisons suggest that tidal pumping in TFZs provides moderate hydrologic storage. Across river networks, storage and exchange rates generally decrease with downstream distance, but TFZs may have slightly higher storage for their size due to the added contributions of tidal pumping. Across inland rivers, for a 2.5 order of magnitude increase in river discharge, only a 1.0 order of magnitude increase in exchange is observed, causing a decline in turnover length (*Cranswick and Cook, 2015*). More studies are needed to assess how hyporheic storage in TFZs compares with other lowland rivers, and future studies should seek to incorporate estimates of hyporheic exchange rates due to other processes such as flow through bedforms.

Even if hyporheic storage volumes in TFZs are similar to zones along non-tidal rivers, the dynamic nature of storage within TFZs is fundamentally different. Bank storage events induced by individual floods or seasonal stage fluctuations only occur intermittently. Storage events due to upstream dam releases occur repeatedly, but magnitudes and frequency vary, and the frequency is usually no more than once daily (*Fritz and Arntzen, 2007; Sawyer et al., 2009*). In contrast, tidal bank storage occurs semidiurnally. Even though magnitudes are similar to other bank storage processes (*Cranswick and Cook, 2015*), repetitive tidal action potentially generates more storage over annual timescales than other individual processes. Bank storage associated with seasonal water table rise in reservoirs has been shown to affect watershed scale flow, and may be an exception over yearly time scales (*Fryar et al. 2006*).

With its semidiurnal frequency, hydraulic storage in TFZs is unique from storage along other lowland rivers, and the influence of that periodic storage on nitrogen export is largely unknown. Long retention times in smaller tributaries have been cited as a major determinant in their ability to reduce nitrogen loads, and as channel size increases downstream, the nitrogen loss rate declines (*Alexander et al.*, 2000). For example, the Mississippi River basin's small tributaries have a large sediment-to-water interface and are estimated to remove more than 90% of nitrogen, while the main stem removes less than 10% (*Alexander et al.*, 2000). As river size increases, the ratio of riverbed area to river volume decreases, along with the potential for nitrogen removal. However, the long transport distances inherent to larger rivers lead to longer residence times, and thus larger rivers are still capable of considerable nitrogen retention (e.g. *Seitzinger et al.*, 2002, *Wollheim et al.* 2006). TFZs represent an expansive component of lowland rivers where the area of the sediment-water interface enlarges at high tide and residence times increase. Thus, tidal rivers may outperform other large rivers in terms of nitrogen retention, and their role in nitrogen fluxes to coasts requires further investigation.

In general, tidal dynamics in TFZs influence hyporheic and groundwater quality in numerous ways. My observations at high tide demonstrate that infiltration enhances dissolved oxygen transfer to microbially active sediments in the riverbed and banks. Tidal water table fluctuations in the riparian aquifer also appear to create a region of increased oxygen concentrations farther from the bank near the water table. Water table fluctuations have previously been shown to enhance dissolved oxygen in shallow groundwater due to imbibition of soil gas (*Wheeler*, 1999). In the absence of tides, oxygen concentrations would likely be uniformly lower in the riverbed and banks, similar

to measurements at low tide. If some of the oxygen I observed at low tide was residual from surface water or soil gas entrapment that occurred during rising tide, oxygen concentrations would be even less in the absence of tides. Thus, tidal fluctuations in the TFZ can enhance the aerobic extent of the hyporheic zone and riparian aquifer.

Oxygen dynamics in the hyporheic zone and riparian aquifer could have several implications for contaminant transport. DO concentrations over the threshold of 1 – 1.5 mg L⁻¹ support aerobic biodegradation of aromatic hydrocarbons (*Wilson and Bower 1997*). Concentrations above this threshold were consistently observed near the channel due to bank storage and near the zone of water table fluctuations over an approximate cross-sectional area of 10 m². These zones would likely be efficient sites of aromatic hydrocarbon removal. *Bianchin et al. (2006)* found a marked decrease in polycyclic aromatic hydrocarbons (PAHs) within the aerobic hyporheic zone of a TFZ and attributed the apparent removal to a high supply of oxygen associated with tidal pumping. At my site, towards the end of bank storage and start of bank release, DO concentrations began to decline, which would presumably facilitate a switch to anaerobic reduction of other contaminants such as nitrate. Reduction of nitrate requires the depletion of DO (*Seitzinger et al., 2006*). Regions of low DO would support denitrification near the end of bank storage events.

5.2 Bank Filtration: An analogous process

A large volume of literature has been published on what can be considered an analogous process to bank storage, bank filtration. In a similar respect, river water flows into the bank due to the hydraulic gradient, though often induced by pumping rather than

natural process. Bank filtration has been shown to attenuate contaminants through filtration, biodegradation, absorption, chemical precipitation, and redox reactions (*Hiscock and Grishcek, 2002*). Attenuation occurs both in the colmation layer, which is the region near the river bed where reduced hydraulic conductivity occurs from the clogging of pores, and along the main flow path towards the borehole (*Hiscock and Grishcek, 2002*). In a tidal setting, the colmation layer may be reduced or absent due to flushing of the pores from tidal pumping. Similar attenuation processes could occur as river water infiltrates into the bank from bank storage, though the colmation layer may be reduced. Bank filtration provides an end member in understanding tidal bank storage that may allow for further insights into contaminant processing.

5.3. Conceptual model of solute transport in TFZs

The timing of surface water-groundwater exchange relative to downstream transport has implications for peak periods of solute storage and release along TFZs. Under base flow conditions, river discharge is relatively static, providing a steady downstream solute transport rate (Figure 5.2.1, T₁ through T₂). Storage begins after tide has begun to rise, when both river velocity and discharge are at their minimum (Figure 5.1, T₃). Solutes that enter the banks at the start of storage would have a longer residence time than solutes that enter at the end of storage (up to 2 hours later, in this case) and thus a greater potential to be transformed in storage zones. With the start of bank release (T₄, Figure 5.2.1), the first water to exfiltrate into the channel would resemble recently infiltrated surface water that has undergone minimal transformation. As release proceeds (T₁ again in Figure 5.1), exfiltrating groundwater would be transformed and differ chemically from surface water. This transformed water would enter the channel when

river discharge is moderate and downstream transport (velocity) is high. Thus, the distinct chemical signal of older exfiltrating water would only experience moderate dilution with surface water in the channel, and this mixed water would be transported rapidly downstream until the start of a new bank storage moment (T_3 , Figure 5.1). The duration of the storage period and extent of chemical transformation should increase in the downstream direction as stage fluctuations increase. The significance of bank storage as a hyporheic process will therefore vary along the TFZ.

5.4. Suggestions for best management of TFZs

TFZs are characterized by unique hydrologic connections, both longitudinally along the channel and laterally across the river-aquifer interface, and management strategies should seek to preserve this connectivity. Structures such as locks and dams limit the upstream extent of tidal fluctuations. The natural lengths of TFZs in unregulated rivers are largely unknown and therefore, it is unclear to what extent dams have truncated TFZs. Removal of dams would allow tides to propagate farther upstream, extending the length of TFZs and increasing hyporheic exchange. To replace traditional dams, new green infrastructure designs have increasingly been proposed and implemented. For example, on White Clay Creek, a tidal capture structure (TCS) has been installed immediately upstream from my study site to augment drinking water supplies under low flow conditions. The TCS remains deflated under normal flow conditions to allow for fish passage and the upstream propagation of tides. As the trend towards greener infrastructure continues, new alternatives to permanent dams and weirs should emerge that promote hydrologic connectivity in TFZs.

Other measures could also be taken to protect hydrologic connectivity. Alluvial riverbeds and banks are often armored with retaining walls, rip rap, and gabion baskets to protect property from erosion. Since populations are concentrated along coasts (*Crossett et al.* 2014), TFZs may be more heavily armored than other inland rivers. Retaining walls and armoring practices in TFZs decrease river-aquifer connectivity. At my site, armored banks would reduce exchange rates by half if lateral connectivity were eliminated, leaving only the bed as a storage zone. Concrete channelization, a common flood management approach, also eliminates tidal pumping, since both the bed and banks are covered with impervious concrete. New flood management strategies such as compound channels are being adopted to reduce flooding while improving hydrologic connectivity and restoring ecological process (*Tompkins and Kondolf*, 2007; *Roni et al.*, 2002). Across the country, the National River Restoration Science Synthesis (NRRSS) is cataloguing restoration projects, including those in TFZs. However, it remains unclear if current restoration efforts are able to restore both the structure and function of streams. In summary, a combination of removing dams and concrete channelization, seeking alternative green technologies, and reducing armoring practices has the potential to restore environmental services provided by TFZs and should be a focus for land managers.

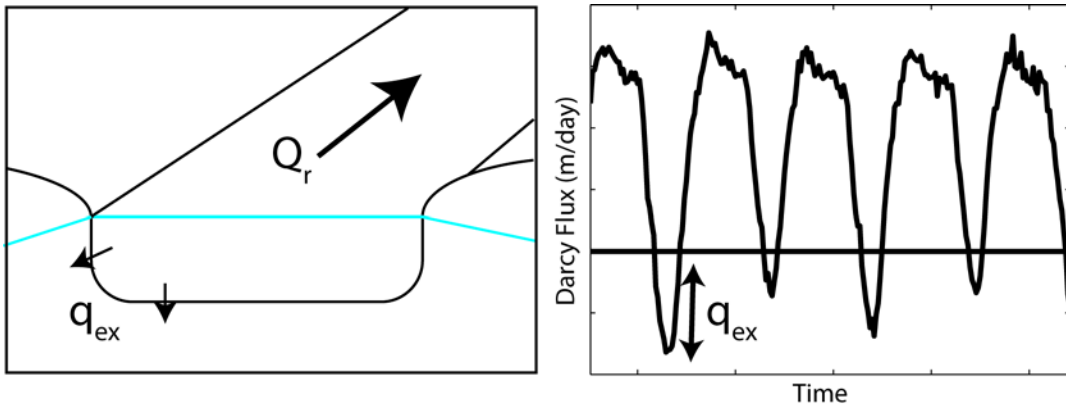


Figure 5.1.1. Conceptual sketch of the components of turnover length.

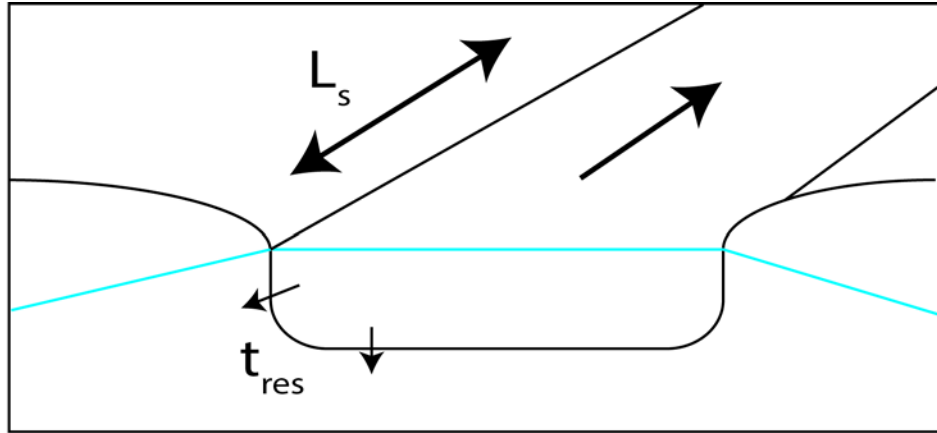


Figure 5.1.2. Conceptual sketch of the components of hydraulic retention.

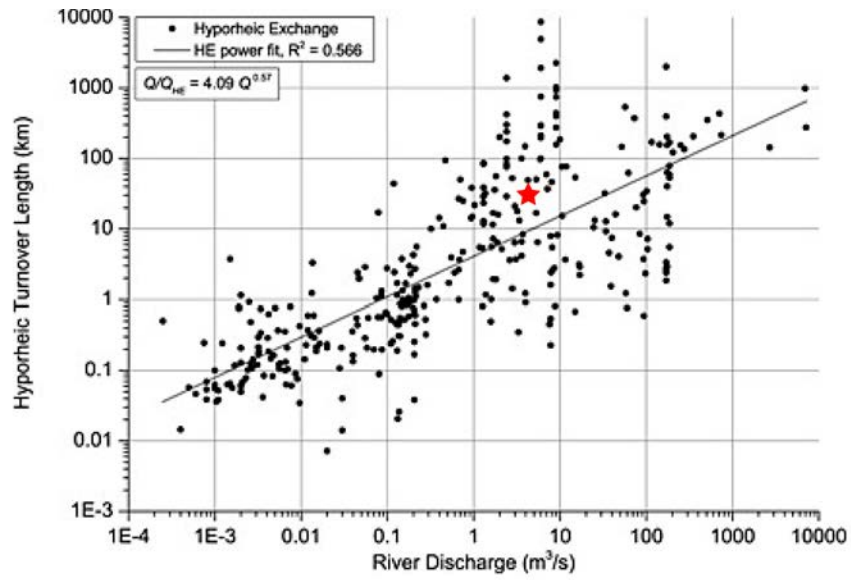


Figure 5.1.3. Turnover length (39 km) at White Clay Creek from bank storage compared to turnover length from all hyporheic processes from the literature (*Cranswick 2015*). The red star denotes White Clay Creek.

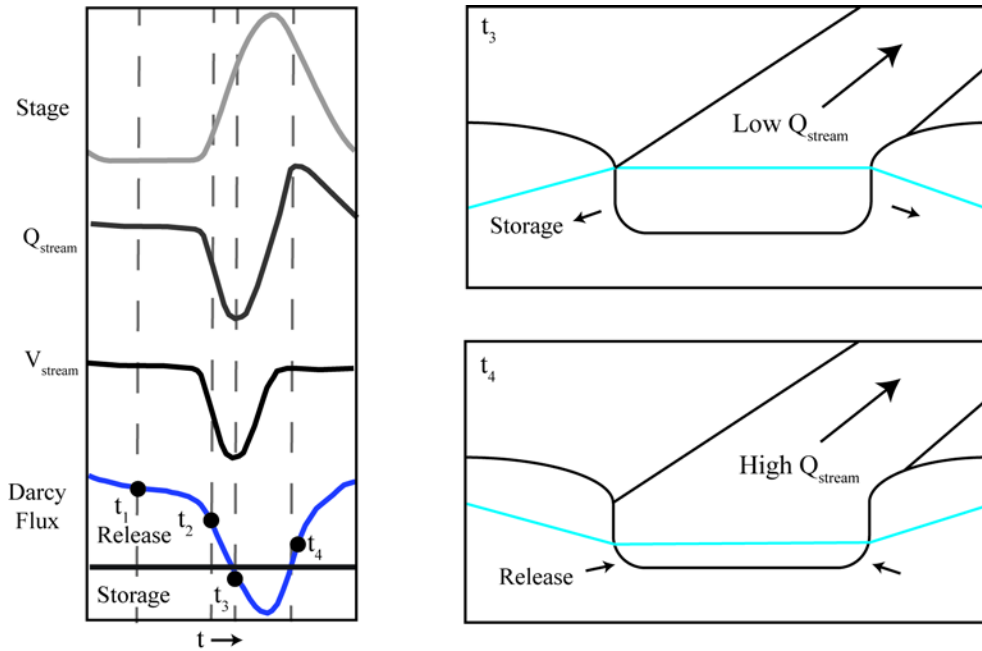


Figure 5.2.1. Conceptual model of competition between downstream transport, hydrologic retention, and geochemical transformation in a TFZ.

Chapter 6. Conclusions

In the TFZ of White Clay Creek at a site 17 km from the Delaware River, tides fluctuate on average 75 cm semidurnally and drive water table fluctuations up to 25 meters from the banks. Tidal bank storage and release exchanges 0.93 m^3 of river water per meter of channel during each tidal cycle. Along the entire TFZ, conservative estimates indicate that 17% of river water flows through hyporheic storage zones due to tidal pumping. Magnitudes of exchange due to tidal pumping are similar to exchange due to all hyporheic processes in non-tidal lowland rivers. Tides drive oxygen rich river water into the surrounding aquifer, while water table fluctuations aerate shallow groundwater. Bank storage water is released during periods of high river velocity and moderate flow, transporting potentially transformed water quickly downstream.

Much coastal river research has focused on pristine marsh creeks with broad tidal floodplains. Incised rivers like White Clay Creek are common within urban and agricultural land use regions, and I have shown that these incised rivers still have tremendous potential to store water and transform contaminants. With at least 17 % of river water exchanging through the hyporheic zone and riparian aquifer, such coastal reaches can impact river chemistry prior to discharge at the coast. Future research should focus on biogeochemical transport and transformations within TFZs. High-resolution, longer-term observations of chemical transport along TFZs and within their riparian aquifers would provide insights that were not captured by my observations from one transect at high and low tide. TFZs stretch for many kilometers and cover a significant proportion of coastal watershed areas. Their potential scaled environmental services are unknown and should be the focus of continued research.

Appendix A. Grain Size Analysis

Core	Depth (cm)	Weighting Tin (g)	Wet (g) Cut Core	Dry (g) Cut Core	Wet (g) Bulk Plug	Dry (g) Bulk Plug	Fraction of Water (g)	Pore Water Volume Fraction	Dry Bulk Density (g/cm ³)	Porosity	D10 (cm)	C	K (m/s)	Mass > 2mm (g)	Macro Organic Matter (g)
C	2-4	1.8803	7.7604	7.6270	2.5808	2.5726	0.0032	0.0032	2.4921	0.4574	0.0502	120	3.03E-03	1.15	0
C	12-14	1.8755	7.6265	7.3657	2.5996	2.5744	0.0097	0.0096	2.4759	0.4618	0.0401	120	1.92E-03	0	0
C	20-22	1.8883	8.8774	6.1675	2.8787	2.5153	0.1262	0.1173	2.2066	0.4143	0.0060	80	2.90E-05	0	0
C	28-30	1.8832	11.3441	9.2950	2.8404	2.6525	0.0662	0.0636	2.3409	0.5083	0.0205	100	4.22E-04	0	0
C	44-46	1.8965	7.8832	5.1325	2.8309	2.4452	0.1362	0.1260	2.1851	0.3626	0.0074	80	4.33E-05	0	0.37
F	6-8	1.8833	5.8374	5.3356	2.5469	2.4639	0.0326	0.0320	2.4201	0.3774	0.0168	80	2.25E-04	0	0
F	22-24	1.8847	8.3292	7.1978	2.4014	2.2980	0.0431	0.0420	2.3951	0.2686	0.0121	80	1.16E-04	0	0
F	30-32	1.8783	6.6721	6.4740	2.5031	2.4830	0.0080	0.0080	2.4800	0.3930	0.0333	110	1.22E-03	0	0
F	36-38	1.9135	7.9919	7.0826	2.8570	2.5085	0.1220	0.1137	2.2158	0.3867	0.0160	80	2.04E-04	0	0
F	44-46	1.9057	6.1236	5.0982	2.7865	2.3407	0.1600	0.1460	2.1350	0.2827	0.0073	70	3.73E-05	0	0
F	54-56	1.8891	4.3705	3.8461	2.6589	2.4863	0.0649	0.0625	2.3438	0.3882	0.0062	70	2.66E-05	0	0
F	60-62	1.8927	6.0152	5.9948	2.4803	2.4772	0.0012	0.0012	2.4969	0.3799	0.0403	110	1.78E-03	0	0
F	74-76	1.8773	5.0537	4.4569	2.5183	2.3955	0.0488	0.0474	2.3816	0.3368	0.0102	80	8.27E-05	0	0
F	78-80	1.8843	5.0938	4.7523	2.8073	2.7028	0.0372	0.0364	2.4090	0.5320	0.0162	80	2.10E-04	0	0
F	84-86	1.8869	7.3964	5.7985	2.7769	2.5322	0.0881	0.0837	2.2908	0.4194	0.0072	60	3.10E-05	0	0
F	96-98	1.8911	7.2831	6.6693	2.6965	2.5827	0.0422	0.0412	2.3971	0.4495	0.0249	120	7.43E-04	0	0
F	102-104	1.8934	7.3809	6.8009	2.6284	2.6076	0.0079	0.0079	2.4803	0.3386	0.0137	100	1.87E-04	0	0.07
F	112-114	1.8932	6.1185	4.8826	2.6400	2.4141	0.0856	0.0814	2.2965	0.4642	0.0066	80	3.53E-05	0	0
F	130-132	1.8850	7.9843	6.9123	2.6244	2.4898	0.0513	0.0498	2.3756	0.4972	0.0189	80	2.85E-04	0	0
F	136-138	1.8872	7.7729	5.8263	2.7910	2.4179	0.1337	0.1238	2.1906	0.4363	0.0058	70	2.37E-05	0	0
F	158-160	1.8925	8.0241	7.1529	2.5253	2.4326	0.0367	0.0359	2.4102	0.4440	0.0177	80	2.50E-04	0	0
F	168-170	1.8779	8.6900	6.8642	2.6492	2.4498	0.0753	0.0720	2.3200	0.4702	0.0052	60	1.61E-05	0	0
F	188-190	1.8779	7.8733	6.2062	2.5781	2.3765	0.0782	0.0747	2.3133	0.4083	0.0056	70	2.21E-05	0	0.02
F	204-206	1.8859	5.5183	5.0428	2.5576	2.4600	0.0382	0.0373	2.4067	0.4720	0.0104	100	1.09E-04	0	0
F	216-218	1.8819	7.5503	6.4417	2.9995	2.7754	0.0747	0.0715	2.3212	0.6425	0.0128	100	1.63E-04	0	0
F	234-236	1.8842	9.7901	7.3316	2.8255	2.5089	0.1121	0.1050	2.2375	0.4492	0.0067	80	3.62E-05	0	0
F	250-252	1.8848	11.0920	9.3830	2.8098	2.6556	0.0549	0.0531	2.3672	0.5542	0.0402	120	1.94E-03	0	0
F	268-270	1.8870	10.8108	9.6643	2.7786	2.6383	0.0505	0.0490	2.3775	0.5402	0.0497	120	2.97E-03	1.35	0
F	270-272	1.8766	8.9355	6.8193	2.9150	2.5189	0.1359	0.1256	2.1859	0.4618	0.0058	80	2.72E-05	0	0
F	278-280	1.8852	8.2560	7.4727	2.7552	2.6390	0.0422	0.0411	2.3972	0.5420	0.0455	120	2.48E-03	1.19	0

Appendix B. Grain Size Distributions

Core/ Location	C	C	C	C	C	F	F	F	F	F
Depth (cm)	2-4	12-14	20-22	28-30	44-46	6-8	22-24	30-32	36-38	44-46
Volume % <1.096	0.00	0	0	0	0	0	0	0	0	0
Volume % <1.259	0.00	0	0.01	0	0	0	0	0	0	0
Volume % <1.445	0.00	0	0.09	0	0.01	0	0.01	0	0.01	0.01
Volume % <1.66	0.00	0	0.31	0	0.16	0.03	0.1	0	0.09	0.22
Volume % <1.905	0.00	0	0.49	0.08	0.32	0.14	0.19	0	0.17	0.37
Volume % <2.188	0.00	0	0.68	0.12	0.48	0.21	0.28	0.06	0.24	0.53
Volume % <2.512	0.02	0.06	0.86	0.17	0.63	0.28	0.36	0.1	0.31	0.68
Volume % <2.884	0.02	0.09	1.03	0.22	0.78	0.34	0.44	0.12	0.37	0.83
Volume % <3.311	0.05	0.11	1.2	0.27	0.93	0.41	0.52	0.15	0.44	0.97
Volume % <3.802	0.07	0.13	1.38	0.33	1.09	0.48	0.6	0.18	0.5	1.11
Volume % <4.365	0.09	0.16	1.57	0.39	1.25	0.54	0.68	0.22	0.56	1.24
Volume % <5.012	0.10	0.2	1.77	0.45	1.41	0.61	0.78	0.26	0.62	1.38
Volume % <5.754	0.13	0.23	1.99	0.52	1.58	0.68	0.88	0.3	0.68	1.51
Volume % <6.607	0.14	0.27	2.23	0.6	1.75	0.75	0.98	0.35	0.75	1.63
Volume % <7.586	0.16	0.31	2.49	0.68	1.92	0.81	1.1	0.4	0.82	1.74
Volume % <8.71	0.19	0.35	2.76	0.76	2.08	0.87	1.22	0.45	0.88	1.85
Volume % <10	0.21	0.38	3.05	0.85	2.23	0.94	1.35	0.5	0.96	1.95
Volume % <11.482	0.23	0.42	3.36	0.93	2.37	1	1.49	0.55	1.03	2.04
Volume % <13.183	0.27	0.46	3.67	1.02	2.5	1.07	1.65	0.6	1.12	2.14
Volume % <15.136	0.30	0.5	3.98	1.11	2.61	1.16	1.84	0.66	1.22	2.24
Volume % <17.378	0.35	0.57	4.28	1.23	2.73	1.29	2.07	0.74	1.36	2.37
Volume % <19.953	0.42	0.67	4.57	1.38	2.86	1.47	2.35	0.87	1.54	2.53
Volume % <22.909	0.52	0.83	4.83	1.58	3.02	1.73	2.69	1.05	1.78	2.76
Volume % <26.303	0.66	1.05	5.04	1.84	3.23	2.09	3.09	1.31	2.1	3.06
Volume % <30.2	0.84	1.36	5.21	2.18	3.49	2.56	3.56	1.67	2.5	3.46
Volume % <34.674	1.06	1.76	5.3	2.6	3.8	3.14	4.06	2.15	2.99	3.94
Volume % <39.811	1.32	2.24	5.3	3.1	4.16	3.82	4.58	2.73	3.55	4.49
Volume % <45.709	1.61	2.77	5.2	3.64	4.53	4.55	5.05	3.39	4.15	5.07
Volume % <52.481	1.89	3.3	4.98	4.21	4.88	5.27	5.42	4.07	4.73	5.6
Volume % <60.256	2.14	3.76	4.65	4.74	5.15	5.9	5.64	4.73	5.24	6.01
Volume % <69.183	2.33	4.1	4.19	5.18	5.28	6.35	5.67	5.27	5.6	6.23
Volume % <79.433	2.42	4.23	3.62	5.48	5.24	6.57	5.47	5.63	5.77	6.19
Volume % <91.201	2.40	4.15	2.99	5.62	4.99	6.49	5.07	5.75	5.72	5.86
Volume % <104.713	2.26	3.84	2.32	5.58	4.54	6.13	4.52	5.6	5.46	5.2
Volume % <120.226	2.02	3.36	1.68	5.4	3.94	5.54	3.9	5.31	5.03	4.46
Volume % <138.038	1.72	2.81	1.11	5.11	3.26	4.8	3.28	4.85	4.49	3.53
Volume % <158.489	1.41	2.3	0.66	4.77	2.58	4.02	2.75	4.34	3.94	2.62
Volume % <181.97	1.12	1.95	0.34	4.41	1.95	3.27	2.36	3.85	3.42	1.77
Volume % <208.93	0.91	1.86	0.15	4.07	1.44	2.65	2.1	3.47	3	1.1
Volume % <239.883	0.81	2.06	0.05	3.74	1.05	2.15	1.95	3.21	2.66	0.6
Volume % <275.423	0.86	2.54	0.02	3.39	0.79	1.8	1.85	3.06	2.4	0.28
Volume % <316.228	1.09	3.24	0.05	3.02	0.62	1.55	1.76	2.98	2.18	0.09
Volume % <363.078	1.49	4.02	0.09	2.61	0.53	1.37	1.63	2.92	1.97	0.04
Volume % <416.869	2.05	4.73	0.11	2.17	0.46	1.22	1.45	2.83	1.75	0.03
Volume % <478.63	2.75	5.24	0.12	1.71	0.41	1.08	1.21	2.67	1.52	0.04
Volume % <549.541	3.53	5.43	0.11	1.25	0.35	0.92	0.93	2.44	1.26	0.05
Volume % <630.957	4.30	5.27	0.08	0.81	0.28	0.74	0.67	2.15	0.99	0.05
Volume % <724.436	4.96	4.78	0.03	0.43	0.18	0.56	0.35	1.81	0.72	0.04
Volume % <831.764	5.41	4.05	0.02	0.18	0.1	0.39	0.12	1.46	0.45	0.02
Volume % <954.993	5.54	3.21	0	0.07	0.03	0.21	0	1.1	0.31	0
Volume % <1096.478	5.28	2.31	0	0	0	0.05	0	0.74	0.25	0
Volume % <1258.925	4.60	1.43	0	0	0	0	0	0.5	0.19	0
Volume % <1445.44	3.57	0.81	0	0	0	0	0	0.3	0.12	0
Volume % <1659.587	2.08	0.23	0	0	0	0	0	0.11	0.06	0
Volume % <1905.461	0.50	0.05	0	0	0	0	0	0.03	0.01	0
Volume % <2000	21.82	0	0	0	0	0	0	0	0	0

Appendix B. (Continued)

Core/ Location	F	F	F	F	F	F	F	F	F	F
Depth (cm)	54-56	60-62	74-76	78-80	84-86	96-98	102-104	112-114	130-132	136-138
Volume % <1.096	0	0	0	0	0	0	0	0	0	0
Volume % <1.259	0.01	0	0	0	0	0	0	0	0	0
Volume % <1.445	0.1	0	0.01	0.01	0.01	0	0.01	0.01	0	0.01
Volume % <1.66	0.32	0	0.12	0.08	0.23	0	0.08	0.25	0	0.26
Volume % <1.905	0.5	0	0.23	0.16	0.38	0.09	0.17	0.42	0.1	0.46
Volume % <2.188	0.69	0	0.33	0.23	0.54	0.14	0.25	0.6	0.16	0.68
Volume % <2.512	0.86	0.05	0.43	0.3	0.7	0.18	0.33	0.77	0.23	0.89
Volume % <2.884	1.02	0.07	0.53	0.37	0.85	0.23	0.41	0.94	0.29	1.1
Volume % <3.311	1.17	0.09	0.62	0.43	1	0.28	0.49	1.1	0.35	1.31
Volume % <3.802	1.33	0.11	0.72	0.5	1.13	0.33	0.57	1.25	0.42	1.51
Volume % <4.365	1.48	0.14	0.83	0.56	1.27	0.38	0.66	1.4	0.49	1.71
Volume % <5.012	1.63	0.17	0.94	0.63	1.39	0.43	0.74	1.54	0.56	1.9
Volume % <5.754	1.8	0.21	1.06	0.7	1.51	0.48	0.82	1.67	0.63	2.09
Volume % <6.607	1.96	0.26	1.19	0.77	1.62	0.53	0.9	1.8	0.7	2.28
Volume % <7.586	2.14	0.31	1.33	0.83	1.73	0.58	0.98	1.93	0.76	2.46
Volume % <8.71	2.33	0.36	1.48	0.89	1.82	0.63	1.04	2.06	0.82	2.63
Volume % <10	2.53	0.4	1.63	0.95	1.92	0.68	1.1	2.19	0.87	2.79
Volume % <11.482	2.74	0.45	1.8	1	2.01	0.73	1.15	2.34	0.92	2.95
Volume % <13.183	2.96	0.49	1.98	1.05	2.11	0.78	1.19	2.5	0.97	3.11
Volume % <15.136	3.19	0.53	2.17	1.11	2.22	0.84	1.22	2.69	1.05	3.26
Volume % <17.378	3.44	0.59	2.4	1.19	2.35	0.93	1.27	2.93	1.18	3.43
Volume % <19.953	3.71	0.68	2.65	1.31	2.52	1.06	1.33	3.2	1.37	3.61
Volume % <22.909	4	0.82	2.95	1.5	2.74	1.24	1.43	3.54	1.65	3.8
Volume % <26.303	4.3	1.03	3.3	1.77	3.02	1.5	1.58	3.92	2.06	4.02
Volume % <30.2	4.61	1.33	3.69	2.16	3.36	1.83	1.79	4.35	2.58	4.25
Volume % <34.674	4.9	1.74	4.13	2.65	3.78	2.24	2.07	4.79	3.22	4.5
Volume % <39.811	5.17	2.26	4.57	3.26	4.24	2.72	2.4	5.22	3.95	4.73
Volume % <45.709	5.36	2.86	4.99	3.93	4.71	3.23	2.78	5.58	4.7	4.93
Volume % <52.481	5.45	3.51	5.32	4.61	5.14	3.74	3.16	5.82	5.4	5.06
Volume % <60.256	5.4	4.13	5.53	5.24	5.47	4.2	3.51	5.88	5.97	5.06
Volume % <69.183	5.17	4.66	5.55	5.71	5.63	4.54	3.79	5.73	6.31	4.92
Volume % <79.433	4.76	5.03	5.36	5.96	5.57	4.74	3.96	5.35	6.38	4.6
Volume % <91.201	4.19	5.19	4.96	5.94	5.26	4.77	4.03	4.76	6.16	4.12
Volume % <104.713	3.48	5.14	4.37	5.64	4.73	4.63	4.01	4	5.67	3.49
Volume % <120.226	2.72	4.92	3.7	5.1	4.02	4.37	3.95	3.16	5	2.79
Volume % <138.038	1.96	4.6	2.99	4.41	3.21	4.03	3.9	2.32	4.24	2.07
Volume % <158.489	1.3	4.29	2.37	3.67	2.43	3.69	3.92	1.57	3.53	1.42
Volume % <181.97	0.77	4.07	1.87	2.97	1.72	3.37	4.03	0.97	2.94	0.87
Volume % <208.93	0.38	3.99	1.54	2.41	1.18	3.11	4.22	0.54	2.52	0.47
Volume % <239.883	0.14	4.05	1.35	2.01	0.8	2.91	4.42	0.26	2.26	0.21
Volume % <275.423	0.01	4.2	1.27	1.79	0.6	2.74	4.56	0.13	2.13	0.04
Volume % <316.228	0	4.35	1.25	1.72	0.53	2.59	4.56	0.07	2.05	0.02
Volume % <363.078	0	4.41	1.24	1.74	0.55	2.45	4.35	0.07	1.98	0.03
Volume % <416.869	0	4.3	1.2	1.8	0.6	2.31	3.92	0.08	1.86	0.04
Volume % <478.63	0	3.97	1.11	1.84	0.63	2.19	3.3	0.1	1.66	0.04
Volume % <549.541	0	3.44	0.97	1.82	0.64	2.12	2.55	0.1	1.4	0.04
Volume % <630.957	0	2.77	0.79	1.72	0.59	2.1	1.78	0.08	1.09	0.03
Volume % <724.436	0	2.05	0.59	1.54	0.5	2.14	0.98	0.04	0.76	0.01
Volume % <831.764	0	1.35	0.39	1.31	0.39	2.19	0.25	0	0.44	0
Volume % <954.993	0	0.62	0.18	1.05	0.27	2.16	0.07	0	0.19	0
Volume % <1096.478	0	0.02	0.04	0.79	0.16	2.08	0	0	0.05	0
Volume % <1258.925	0	0	0	0.54	0.11	1.96	0	0	0	0
Volume % <1445.44	0	0	0	0.28	0.06	1.61	0	0	0	0
Volume % <1659.587	0	0	0	0.05	0.03	0.97	0	0	0	0
Volume % <1905.461	0	0	0	0.01	0.01	0.24	0	0	0	0
Volume % <2000	0	0	0	0	0	0	0	0	0	0

Appendix B. (Continued)

Core/ Location	F	F	F	F	F	F	F	F	F	F
Depth (cm)	158-160	168-170	188-190	204-206	216-218	234-236	250-252	268-270	270-272	278-280
Volume % <1.096	0	0	0	0	0	0	0	0.00	0	0.00
Volume % <1.259	0	0.02	0.01	0	0	0.01	0	0.00	0.02	0.00
Volume % <1.445	0	0.15	0.1	0.01	0.01	0.1	0	0.00	0.12	0.00
Volume % <1.66	0	0.42	0.33	0.13	0.07	0.28	0	0.00	0.35	0.00
Volume % <1.905	0.13	0.64	0.53	0.24	0.16	0.43	0	0.00	0.54	0.00
Volume % <2.188	0.19	0.86	0.73	0.35	0.25	0.58	0	0.01	0.73	0.00
Volume % <2.512	0.26	1.08	0.93	0.45	0.33	0.73	0.05	0.03	0.92	0.04
Volume % <2.884	0.32	1.28	1.12	0.55	0.42	0.88	0.08	0.06	1.09	0.06
Volume % <3.311	0.38	1.48	1.32	0.65	0.5	1.03	0.1	0.07	1.26	0.07
Volume % <3.802	0.45	1.68	1.53	0.75	0.59	1.18	0.12	0.10	1.43	0.08
Volume % <4.365	0.52	1.89	1.76	0.85	0.68	1.34	0.15	0.11	1.59	0.10
Volume % <5.012	0.59	2.12	2.01	0.94	0.77	1.51	0.18	0.13	1.77	0.12
Volume % <5.754	0.66	2.36	2.29	1.04	0.87	1.68	0.21	0.15	1.95	0.14
Volume % <6.607	0.72	2.62	2.6	1.13	0.96	1.86	0.24	0.17	2.13	0.16
Volume % <7.586	0.79	2.9	2.93	1.21	1.05	2.04	0.28	0.19	2.32	0.19
Volume % <8.71	0.85	3.19	3.27	1.29	1.14	2.22	0.32	0.21	2.5	0.22
Volume % <10	0.91	3.48	3.62	1.36	1.21	2.41	0.36	0.23	2.68	0.25
Volume % <11.482	0.97	3.77	3.97	1.42	1.29	2.6	0.4	0.26	2.85	0.28
Volume % <13.183	1.03	4.04	4.3	1.48	1.36	2.8	0.44	0.29	3	0.31
Volume % <15.136	1.1	4.27	4.59	1.55	1.43	3.01	0.49	0.33	3.13	0.35
Volume % <17.378	1.2	4.47	4.83	1.65	1.52	3.26	0.57	0.38	3.25	0.40
Volume % <19.953	1.35	4.62	5.01	1.78	1.64	3.52	0.68	0.45	3.35	0.47
Volume % <22.909	1.56	4.71	5.13	1.96	1.81	3.82	0.85	0.55	3.45	0.57
Volume % <26.303	1.86	4.75	5.16	2.22	2.03	4.14	1.09	0.68	3.56	0.71
Volume % <30.2	2.25	4.74	5.11	2.56	2.33	4.47	1.41	0.84	3.69	0.92
Volume % <34.674	2.74	4.68	4.99	2.98	2.71	4.8	1.82	1.03	3.83	1.19
Volume % <39.811	3.31	4.58	4.79	3.46	3.15	5.1	2.32	1.25	3.99	1.52
Volume % <45.709	3.94	4.42	4.52	3.97	3.62	5.32	2.88	1.48	4.15	1.92
Volume % <52.481	4.56	4.21	4.18	4.44	4.08	5.43	3.45	1.70	4.28	2.34
Volume % <60.256	5.12	3.94	3.78	4.82	4.48	5.39	3.99	1.90	4.35	2.76
Volume % <69.183	5.55	3.59	3.32	5.04	4.76	5.19	4.43	2.04	4.31	3.12
Volume % <79.433	5.78	3.18	2.82	5.05	4.88	4.81	4.73	2.11	4.14	3.38
Volume % <91.201	5.79	2.7	2.29	4.84	4.82	4.28	4.85	2.09	3.84	3.49
Volume % <104.713	5.58	2.18	1.76	4.41	4.6	3.62	4.8	1.98	3.4	3.46
Volume % <120.226	5.19	1.67	1.27	3.83	4.25	2.92	4.61	1.80	2.87	3.27
Volume % <138.038	4.68	1.18	0.84	3.19	3.84	2.21	4.34	1.54	2.3	2.96
Volume % <158.489	4.16	0.78	0.51	2.58	3.46	1.57	4.07	1.25	1.76	2.59
Volume % <181.97	3.66	0.46	0.27	2.08	3.15	1.05	3.87	0.96	1.29	2.20
Volume % <208.93	3.25	0.25	0.12	1.74	2.96	0.66	3.77	0.68	0.95	1.87
Volume % <239.883	2.93	0.13	0.09	1.57	2.87	0.39	3.76	0.46	0.73	1.62
Volume % <275.423	2.68	0.07	0.09	1.55	2.86	0.23	3.82	0.34	0.64	1.49
Volume % <316.228	2.47	0.06	0.11	1.64	2.87	0.16	3.89	0.37	0.63	1.50
Volume % <363.078	2.26	0.07	0.14	1.77	2.83	0.15	3.92	0.59	0.68	1.63
Volume % <416.869	2.02	0.08	0.17	1.9	2.71	0.16	3.85	1.06	0.73	1.86
Volume % <478.63	1.75	0.09	0.18	1.98	2.47	0.17	3.66	1.77	0.75	2.16
Volume % <549.541	1.44	0.08	0.18	1.99	2.12	0.18	3.35	2.69	0.73	2.48
Volume % <630.957	1.13	0.05	0.16	1.92	1.7	0.16	2.95	3.74	0.65	2.77
Volume % <724.436	0.82	0.02	0.11	1.79	1.25	0.11	2.49	4.79	0.53	2.97
Volume % <831.764	0.52	0	0.06	1.61	0.81	0.04	2.02	5.67	0.39	3.07
Volume % <954.993	0.25	0	0.05	1.38	0.35	0	1.55	6.18	0.24	3.02
Volume % <1096.478	0.14	0	0.03	1.1	0	0	1.09	6.19	0.14	2.79
Volume % <1258.925	0.1	0	0	0.78	0	0	0.77	5.59	0.04	2.37
Volume % <1445.44	0.07	0	0	0.58	0	0	0.54	4.45	0	1.81
Volume % <1659.587	0.04	0	0	0.34	0	0	0.3	2.63	0	1.04
Volume % <1905.461	0.01	0	0	0.08	0	0	0.07	0.64	0	0.25
Volume % <2000	0	0	0	0	0	0	0	25.81	0	25.65

Appendix C. Low Tide Groundwater and Surface Water Chemistry Parameters

Well	Depth	Time	pH	Conductivity ($\mu\text{s}/\text{cm}$)	DO (mg/L)	Temp C ^o	Date
A	0.12	11:19	6.84	473.3	0.33	19.6	6/16/2014
A	0.25	11:16	6.73	406.3	1.26	18.8	6/16/2014
A	0.5	11:14	6.44	330.8	0.64	17.9	6/16/2014
A	0.75	11:12	5.85	226.1	0.64	17.5	6/16/2014
A	1	11:09	5.8	217.7	0.61	16.9	6/16/2014
B	0.12	11:43	6.73	401.8	0.63	19.4	6/16/2014
B	0.25	11:40	6.56	401.9	0.42	19.1	6/16/2014
B	0.5	11:37	6.27	348.2	0.47	19.2	6/16/2014
B	0.75	11:34	5.8	261.2	0.4	17.5	6/16/2014
B	1	11:30	5.77	248	0.48	16.6	6/16/2014
C	0.12	11:59	6.4	330	1.25	20	6/16/2014
C	0.25	11:56	6.21	307.5	1.86	19	6/16/2014
C	0.5	11:54	6.07	278.3	1.27	17.8	6/16/2014
C	0.75	11:52	5.96	263.7	0.31	17.3	6/16/2014
C	1	11:49	5.78	243.1	0.39	16.3	6/16/2014
D	2	10:37	5.88	259.4	3.34	14.8	6/16/2014
D	2.5	10:41	6.38	493	0.64	14.5	6/16/2014
D	3	10:45	5.97	286.5	0.6	13.2	6/16/2014
E	2.5	10:51	5.67	265.9	0.36	12.9	6/16/2014
E	3	10:54	5.94	257.8	0.29	13.1	6/16/2014
F	2.5	11:00	5.64	251.8	0.33	12.2	6/16/2014
F	3	10:58	5.72	226.7	0.5	12	6/16/2014
G	2.5	12:09	5.89	203.2	1.04	17.8	6/16/2014
G	3	12:06	6.29	252.4	2.75	18.9	6/16/2014
H	2.5	12:19	5.97	260.4	0.57	15.2	6/16/2014
H	3	12:16	5.93	250.1	0.58	15.3	6/16/2014
S		11:21	7.69	351.8	8.75	20.6	6/16/2014

Appendix D. High Tide Groundwater and Surface Water Chemistry Parameters

Well	Depth	Time	pH	Conductivity ($\mu\text{s}/\text{cm}$)	DO (mg/L)	Temp C ^o	Date
A	0.12	15:34	6.39	341.1	1.44	22.6	6/16/2014
A	0.25	15:32	6.24	314.8	0.85	21.5	6/16/2014
A	0.5	15:28	6.06	279.1	0.35	18.8	6/16/2014
A	0.75	15:25	5.94	260.8	0.3	18.3	6/16/2014
A	1	15:22	5.79	245.2	0.33	17.6	6/16/2014
B	0.12	15:17	6.7	401	0.28	21.1	6/16/2014
B	0.25	15:14	6.51	405.2	0.3	20.1	6/16/2014
B	0.5	15:11	6.24	360.5	1.41	18.7	6/16/2014
B	0.75	15:09	5.77	265	0.3	18.4	6/16/2014
B	1	15:06	5.75	255.7	0.37	18.4	6/16/2014
C	0.12	15:34	6.39	341.1	1.44	22.6	6/16/2014
C	0.25	15:32	6.24	314.8	0.85	21.5	6/16/2014
C	0.5	15:28	6.06	279.1	0.35	18.8	6/16/2014
C	0.75	15:25	5.94	260.8	0.3	18.3	6/16/2014
C	1	15:22	5.79	245.2	0.33	17.6	6/16/2014
D	1.7	15:51	5.85	234.5	5	18	6/16/2014
D	2	15:49	5.95	245.5	1.75	15	6/16/2014
D	2.5	15:46	6.36	486	0.39	14.3	6/16/2014
D	3	15:46	6	289.7	0.87	13.3	6/16/2014
E	2	16:03	5.54	288.5	1.03	14	6/16/2014
E	2.5	15:59	5.64	262.9	0.52	13.7	6/16/2014
E	3	15:55	5.89	257.6	0.41	13.8	6/16/2014
F	2.5	16:08	5.6	252.8	0.4	13.1	6/16/2014
F	3	16:05	5.74	229.2	1.71	13.7	6/16/2014
G	2.5	16:16	5.85	200.5	1.09	16.1	6/16/2014
G	3	16:12	6.17	255.6	1.71	14.3	6/16/2014
H	2.5	16:24	6.03	275.5	0.55	15.3	6/16/2014
H	3	16:20	5.91	251.9	0.56	14.6	6/16/2014
S		15:19	7.54	351.2	9.04	23.4	6/16/2014

Appendix E: Piezometer Data

Well	D	E	E	G	H
Ground (m)	-0.07	0.11	-0.09	-0.01	-0.28
Top of Casing (m)	0.49	0.34	0.35	0.58	0.04
Top of Screen (m)	-1.09	-1.23	-1.23	-0.99	-1.53
Bottom of Screen (m)	-2.45	-2.59	-2.59	-2.35	-2.89
Top of Casing to Top of Screen (m)	1.57	1.57	1.57	1.57	1.57
Top of Screen to Bottom of Screen (m)	1.36	1.36	1.36	1.36	1.36

Appendix F: Field Photographs



Photograph 1: Sampling pore water to describe riparian aquifer chemistry.



Photograph 2: Sampling of vertical head gradients at low tide using a manometer board.



Photograph 3: Using an Acoustic Doppler Current Profiler to collect stream discharge over a tidal cycle.



Photograph 4: View of the Hale Byrnes House from the field site.

Appendix G. Water Table Fluctuation Logs

Explanation

The data set includes all recorded water table and stage fluctuations and is included as additional data.

REFERENCES

- Alexander, R. B., et al. (2000). "Effect of stream channel size on the delivery of nitrogen to the Gulf of Mexico." *Nature* 403(6771): 758-761.
- Alexander R.B., et al. (2009). "Dynamic modeling of nitrogen losses in river networks unravels the coupled effects of hydrological and biogeochemical processes." *Biogeochemistry*, 93:91-116
- Anderson, W.P., Storniolo, R.E., Rice, R.S. (2011). "Bank thermal storage as a sink of temperature surges in urbanized streams." *Journal of Hydrology* 409: 525-537.
- Bates, P. D., et al. (2000). "Numerical simulation of floodplain hydrology." *Water Resources Research*: 36(9): 2517-2529.
- Bianchin, M., et al. (2006). "Anaerobic degradation of naphthalene in a fluvial aquifer: A radiotracer study." *Journal of Contaminant Hydrology* 84(3): 178-196.
- Bianchin, M. S., L. and Smith, R.D. Beckie (2010). "Quantifying hyporheic exchange in a tidal river using temperature time series." *Water Resources Research* 46(7): W07507.
- Bianchin, M. S., L. and Smith, R.D. Beckie (2011). "Defining the hyporheic zone in a large tidally influenced river." *Journal of Hydrology* 406: 16-29.
- Boano, F., et al. (2006). "Sinuosity-driven hyporheic exchange in meandering rivers." *Geophysical Research Letters* 33(18): L18406.
- Boano, F., et al. (2007). "Bedform-induced hyporheic exchange with unsteady flows." *Advances in Water Resources* 30(1): 148-156.
- Bohlke, J.K., and Denver, J.M. (1995). "Combined use of groundwater dating, chemical and isotopic analyses to resolve the history and fate of nitrate contamination in 2 agricultural watersheds, Atlantic Coastal Plain, Maryland." *Water Resources Research* 31(9): 2319-2339.
- Brunke, M., and Gonser T. (1997). "The ecological significance of exchange processes between rivers and groundwater." *Freshwater Biology* 37(1): 1-33.
- Cardenas, M. B., et al. (2004). "Impact of heterogeneity, bed forms, and stream curvature on subchannel hyporheic exchange." *Water Resources Research* 40(8): W08307.
- Chiang, C.Y., Salanitro, J.P., Chai, E.Y., Colthart, J.D., Klein, C.L. (1989). "Aerobic biodegradation of benzene, toluene and xylene in a sandy aquifer-data analysis and computer modeling." *Ground Water* 27:823-834.

- Cranswick, R. H. and Cook P. G. (2015). "Scales and magnitude of hyporheic, river-aquifer and bank storage exchange fluxes." *Hydrological Processes*.
- Crossett, K., et al. (2014). "National coastal population report, population trends from 1970 to 2020." National Oceanic and Atmospheric Administration, Department of Commerce, developed in partnership with the US Census Bureau.
- Dangelo, D. J., et al. (1993). "Transient storage in Appalachian and Cascade mountain streams as related to hydraulic characteristics." *Journal of the North American Benthological Society* 12(3): 223-235.
- Ensign, S. H., Piehler, M. F., Doyle, M. W. (2008). "Riparian zone denitrification affects nitrogen flux through a tidal freshwater river." *Biogeochemistry* 91(2-3): 133-150.
- Fetter, C.W. (2001). "Applied Hydrogeology." 4th ed., Prentice Hall, Englewood Cliffs, NJ.
- Findlay, S. (1995). "Importance of surface-subsurface exchange in stream ecosystems - the hyporheic zone." *Limnology and Oceanography* 40(1): 159-164.
- Francis, B. A., et al. (2010). "Water table dynamics and groundwater-surface water interaction during filling and draining of a large fluvial island due to dam-induced river stage fluctuations." *Water Resources Research* 46: 5.
- Fryar, A.E., et al. (2006). "Groundwater flow and reservoir management in a tributary watershed along Kentucky Lake." *Journal of the Kentucky Academy of Science* 68(1): 11-23.
- Freeze, R.A. and Cherry, J.A. (1979). "Groundwater." Prentice-Hall, Inc., Englewood Cliffs, NJ. 604 pp.
- Fritz, B. G., and Arntzen E. V. (2007). "Effect of rapidly changing river stage on uranium flux through the hyporheic zone." *Ground Water* 45(6): 753-760.
- Graf, W.L. (2006). "Downstream hydrologic and geomorphic effects of large dams on American rivers." *Geomorphology* 79(3-4): 336-360.
- Gu C.H., et al. (2012). "Riparian biogeochemical hot moments induced by stream fluctuations." *Water Resources Research* 48: 1-17.
- Harvey, J.W., et al. (2003). "Predicting changes in hydrologic retention in an evolving semi-arid alluvial stream." *Advances in Water Resources* 26(9): 939-950.
DOI:10.1016/s0309-1708(03)00085-x.

Hazen, A. (1893). "Some physical properties of sand and gravels, with special reference to their use in filtration." Twenty Fourth Annual Report, State Board of Health of Massachusetts: 541-556.

Hill, A. R., et al. (2000). "Subsurface denitrification in a forest riparian zone: Interactions between hydrology and supplies of nitrate and organic carbon." *Biogeochemistry* 51(2): 193-223.

Hiscick, K.M., and Grischek, T. (2002). "Attenuation of groundwater pollution by bank filtration." *Journal of Hydrology* 266:139-144.

IPCC (2014). Summary for Policymakers. Climate Change 2014: Impacts, Adaptation, and Vulnerability. Part A: Global and Sectoral Aspects. Contribution of Working Group II to the Fifth Assessment Report of the Intergovernmental Panel on Climate Change. C. B. Field, V. R. Barros, D. J. Dokken et al. Cambridge, United Kingdom, and New York, NY, USA, Cambridge University Press: 1-32.

Kasahara, T. and Hill, A.R. (2007). "Lateral hyporheic zone chemistry in an artificially constructed gravel bar and a re-meandered stream channel, southern Ontario, Canada." *J. Am. Water Resources Association* 43(5): 1257-1269.

Loheide, S. P., and Lundquist J. D. (2009). "Snowmelt-induced diel fluxes through the hyporheic zone." *Water Resources Research* 45(7): W07404.

Moffett, K. B., et al. (2012). "Salt marsh ecohydrological zonation due to heterogeneous vegetation-groundwater-surface water interactions." *Water Resources Research* 48: 22.

Morrice, J. A., et al. (1997). "Alluvial characteristics, groundwater-surface water exchange and hydrological retention in headwater streams." *Hydrological Processes* 11(3): 253-267.

Mulholland, P. J., et al. (2008). "Stream denitrification across biomes and its response to anthropogenic nitrate loading." *Nature* 452(7184): 202-205.

Packman, A., et al. (2004). "Hyporheic exchange with gravel beds: Basic hydrodynamic interactions and bedform-induced advective flows." *Journal of Hydraulic Engineering-ASCE* 130(7): 647-656.

Packman, A. I., et al. (2006). "Development of layered sediment structure and its effects on pore water transport and hyporheic exchange." *Water, Air, & Soil Pollution* 6(5): 433-442.

Pinder, G.F., and Sauer, S.P. (1971). "Numerical simulation of flood wave modification due to bank storage effects." *Water Resources Research* 7(1): 63-70.

- Ramsey, K.W. (2005). Geologic Map of New Castle County, Delaware: Delaware Geological Survey Geologic Map 13, scale 1:100,000
- Rivett, M. O., et al. (2008). "Nitrate attenuation in groundwater: A review of biogeochemical controlling processes." *Water Resources* 42: 4215-4232.
- Roni, P., et al. (2002). "A review of stream restoration techniques and a hierarchical strategy for prioritizing restoration in Pacific northwest watersheds." *North American Journal of Fisheries Management* 22(1): 1-20.
- Ryther, J.H., and Dunstan, W.M., (1971). "Nitrogen, phosphorous, and eutrophication in coastal marine environment." *Science* 171(3975):1008-1013.
- Sawyer, A. H., et al. (2009). "Impact of dam operations on hyporheic exchange in the riparian zone of a regulated river." *Hydrological Processes* 22: 2129-2137.
- Schuchardt, B., et al. (1993). "The tidal freshwater reach of the Weser estuary: Riverine or estuarine?" *Netherlands Journal of Aquatic Ecology* 27(2-4): 215-226.
- Schultz, G., and Ruppel C. (2002). "Constraints on hydraulic parameters and implications for groundwater flux across the upland–estuary interface." *Journal of Hydrology* 260(1–4): 255-269.
- Seitzinger, S.P. et al. (2002). "Nitrogen retention in rivers: Model development and application to watersheds in the Northeastern USA." *Biogeochemistry*, 57(1): 199-237.
- Seitzinger, S., et al. (2006). "Denitrification across landscapes and waterscapes: A synthesis." *Ecological Applications* 16(6): 2064-2090.
- Squillace, P.J. (1996). "Observed and simulated movement of bank-storage water." *Groundwater* 34(1):121-134.
- Squillace, P.J., et al. (1993). "Groundwater as a nonpoint-source of atrazine and deethylatrazine in a river during base-flow conditions." *Water Resources Research* (29)6:1719-1729.
- Stanford, J. A., and Ward J.V. (1988). "The hyporheic habitat of river ecosystems." *Nature* 335(6185): 64-66.
- Thibodeaux, L. J., and Boyle J.L. (1987). "Bedform-generated convective-transport in bottom sediment." *Nature* 325(6102): 341-343.
- Tompkins, M. R., and Kondolf G.M. (2007). "Systematic postproject appraisals to maximise lessons learned from river restoration projects: Case study of compound channel restoration projects in Northern California." *Restoration Ecology* 15(3): 524-537.

Turner, R. E. and Rabalais, N.N. (1994). "Coastal Eutrophication near the Mississippi River delta." *Nature* 368(6472):619-621.

Valett, H. M., et al. (1996). "Parent lithology, surface-groundwater exchange, and nitrate retention in headwater streams." *Limnology and Oceanography* 41(2): 333-345.

Wheeler, B. D. (1999), Water and plants in freshwater wetlands, in *Eco-Hydrology: Plants and Water in Terrestrial and Aquatic Environments*, edited by A. J. Baird and R. L. Wilby, pp. 127–180, Routledge, London, U. K.

Wilson, A. M., and Gardner, L.R. (2006). "Tidally driven groundwater flow and solute exchange in a marsh: Numerical simulations." *Water Resources Research* 42: 1-9.

Wilson, L. P. and Bouwer, E.J. (1997). "Biodegradation of aromatic compounds under mixed oxygen/denitrifying conditions: A review." *J. of Industrial Microbiology & Biotechnology* 18(2):116-130.

Woessner, W.W. (2000). "Stream and fluvial plain ground water interactions: rescaling hydrogeologic thought." *Groundwater* 38(3): 423-429.

Wollheim, W.M., C.J. Vörösmarty, B.J. Peterson, S.P. Seitzinger, & C.S. Hopkinson (2006), Relationship between river size and nutrient removal, *Geophysical Research Letters*, 33, L06410, doi: 10.1029/2006GL025845

Wondzell, S.M. (2011). "The role of the hyporheic zone across stream networks." *Hydrological Processes* 25(22): 3525-3532.

Xin, P., Yuan, L.R., Li, L., Barry, D.A. (2011). "Tidally driven multiscale pore water flow in a creek-marsh system." *Water Resources Research* 47(7): W07534.

CURRICULUM VITA

Cole T. Musial

University of Kentucky
Dept. of Earth and Environmental Sciences
Lexington, KY 40560-0053

Education

2013: B.A. Environmental Sciences, Capital University, Bexley, Ohio.

Graduate Study at the University of Kentucky

Cognate Area: Hydrogeology

Thesis: Dynamic surface water-groundwater exchange in tidal freshwater zones: Insights from the Christina River Basin (Delaware, USA)

Thesis Advisor: Audrey H. Sawyer, Assistant Professor

Teaching Experience

2013 – 2015: Teaching Assistant for Earthquakes and Volcanos, Hydrology and Water Resources, Endangered Planet, Geology for Teachers, University of Kentucky, Lexington, KY

2010 – 2013: Teaching Assistant for Introduction to Biology, Capital University, Bexley, OH

Research Grants

GSA Student Research Grant

Ferm Fund award of UK Dept. of Earth and Environmental Science

GSA Southeastern Section Student Travel Grant

Woods and Water Academic Scholarship

Boyd Undergraduate Scholarship Award award of Capital University

Professional Experience

2010 Cleveland Museum of Natural History, Vertebrate Zoology Intern

2011 Northeast Ohio Regional Sewer District, Water Quality and Industrial Surveillance Division – Intern

2012 Northeast Ohio Regional Sewer District, Water Quality and Industrial Surveillance Division – Intern

2015: Ohio Environmental Protection Agency – Intern

Abstracts

Musial, C., Sawyer A., Barnes R., Bray S., Knights D., (2014). Dynamic surface water-groundwater interactions in a tidally influenced river. Annual Meeting of the Geological Society of America (Oral)

Musial, C., (2013). A Comprehensive Hydrologic Cycle Analysis of the Merle and Margaret Primmer Outdoor Learning Center Wetland. National Conference on Undergraduate Research. (Poster)

Musial, C., (2011). Genetic discrimination of species using DNA bar coding. Capital University Symposium on Undergraduate Research. (Poster)